

AperTO - Archivio Istituzionale Open Access dell'Università di Torino

Low-degree spline quasi-interpolants in the Bernstein basis

This is a pre print version of the following article:

Original Citation:

Availability:

This version is available <http://hdl.handle.net/2318/1916370> since 2025-01-14T14:05:43Z

Published version:

DOI:10.1016/j.amc.2023.128150

Terms of use:

Open Access

Anyone can freely access the full text of works made available as "Open Access". Works made available under a Creative Commons license can be used according to the terms and conditions of said license. Use of all other works requires consent of the right holder (author or publisher) if not exempted from copyright protection by the applicable law.

(Article begins on next page)

Low-degree spline quasi-interpolants in the Bernstein basis

D. Barrera^{a,*}, S. Eddargani^b, M. J. Ibáñez^a, S. Remogna^c

^a*Department of Applied Mathematics, University of Granada, Campus de Fuentenueva s/n, 18071 Granada, Spain*

^b*Department of Mathematics, University of Rome Tor Vergata, Rome, Italy*

^c*Department of Mathematics, University of Torino, via C. Alberto, 10, 10123 Torino, Italy*

Abstract

In this paper we propose the construction of univariate low-degree quasi-interpolating splines in the Bernstein basis, considering C^1 and C^2 smoothness, specific polynomial reproduction properties and different sets of evaluation points. The splines are directly determined by setting their Bernstein-Bézier coefficients to appropriate combinations of the given data values. Moreover, we get quasi-interpolating splines with special properties, imposing particular requirements in case of free parameters. Finally, we provide numerical tests showing the performances of the proposed methods.

Keywords: Quasi-interpolation, Bernstein basis, Bézier-ordinates.

1. Introduction

It is well-known that the approximation of functions and data in one and high dimensions is very important and arises from many mathematical problems and scientific applications. In such a context, quasi-interpolation is a useful tool for its peculiar features: see e.g. the book [1] for a general overview on the application of quasi-interpolation for solving integral equations [2, 3], for dealing with problems for partial differential equations [4, 5, 6, 7] and fractional differential problems [8, 9], for modeling terrain [10], and other standard problems in numerical analysis [11].

Indeed, the construction of classical approximants of a given data set or a function often requires the resolution of linear systems. Spline quasi-interpolants are local approximants avoiding this problem, so they are very convenient in practice. In general, a quasi-interpolant for a given function f is obtained as linear combination of some elements of a suitable set of basis functions. In order to achieve local control, these basis functions are required to be positive, to ensure stability and to have small local supports. Bernstein polynomial bases fulfill these requirements. In fact, Bernstein polynomial bases are extremely helpful mathematical tools as they are simply defined, easily implemented on computer systems and they represent a wide range of functions and curves. Among the most powerful properties of these polynomials are the partition of unity and the fact that they are non-negative.

Taking into account the aforementioned requirements, in this work we propose the construction of univariate quasi-interpolating splines of degree 2, 3, 4 and 5 in the Bernstein basis, considering C^1 and C^2 smoothness, specific polynomial reproduction properties and different sets of evaluation points. The splines are directly determined by setting their Bernstein-Bézier coefficients to appropriate combinations of the given data values (see also [12, 13, 14] where data/function approximation in the bivariate case is faced by using such a technique).

Here is an outline of the paper. In Section 2 we give some preliminaries and we introduce the notations used throughout the paper. Then, in Sections 3 and 4 we construct and study quadratic and cubic quasi-interpolating splines, respectively. Finally, in Section 5 the quartic and quintic cases are addressed. In each section, fixing the degree, we propose different quasi-interpolating splines,

* corresponding author.

Email addresses: dbarrera@ugr.es (D. Barrera), eddargani@mat.uniroma2.it (S. Eddargani), mibanez@ugr.es (M. J. Ibáñez), sara.remogna@unito.it (S. Remogna)

varying the smoothness, the polynomial reproduction properties and the set of evaluation points necessary to construct them, and we get several possibilities imposing also particular requirements in case of free parameters. Moreover, in each section we provide numerical tests showing the performances of the proposed methods.

2. Preliminaries

Throughout this paper, we consider the uniform partition $a + h\mathbb{Z}$ of the real line given by the knots $x_i := a + i h$, $i \in \mathbb{Z}$, with $a \in \mathbb{R}$ and $h > 0$, yielding subintervals $I_i := [x_i, x_{i+1}]$, and the space $S_d^r := S_d^r(a + h\mathbb{Z})$ of C^r polynomial splines of degree d on \mathbb{R} defined by

$$S_d^r := \{s \in C^r(\mathbb{R}) : s_i := s|_{I_i} \in \mathbb{P}_d, i \in \mathbb{Z}\},$$

where $r \in \mathbb{N}$ and \mathbb{P}_d stands for the space of polynomials of degree less than or equal to $d \geq 2$.

Since each point $x \in I_i$ can be expressed from its barycentric coordinates $(1-t, t)$, $0 \leq t \leq 1$, with respect to I_i as $x = (1-t)x_i + t x_{i+1}$, then s_i can be represented in terms of the Bernstein polynomials relative to I_i , i.e., $\mathfrak{B}_{\alpha,i}$ where $\alpha := (\alpha_1, \alpha_2) \in \mathbb{N}_0^2$ with length $|\alpha| := \alpha_1 + \alpha_2 = d$. They are defined as

$$\mathfrak{B}_{\alpha,i}(x) := \frac{d!}{\alpha_1! \alpha_2!} (1-t)^{\alpha_1} t^{\alpha_2}, x \in I_i,$$

with $t := \frac{x-x_i}{h}$. Then, the Bernstein-Bézier (BB-) representation of s_i is the unique linear combination

$$s_i = \sum_{|\alpha|=d} b_{\alpha,i} \mathfrak{B}_{\alpha,i}, \quad (1)$$

whose coefficients $b_{\alpha,i}$ are said to be the Bézier (B-) ordinates or BB-coefficients of s_i . They are naturally linked to the domain points $\xi_{\alpha,i} := \frac{\alpha_1}{d} x_i + \frac{\alpha_2}{d} x_{i+1}$ in I_i determined by the barycentric coordinates $(\frac{\alpha_1}{d}, \frac{\alpha_2}{d})$, $|\alpha| = d$. Let $\Xi_{d,i} := \{\xi_{\alpha,i} \in I_i : |\alpha| = d\}$ be the subset of all domain points relative to I_i , and let $\Xi_d := \bigcup_{i \in \mathbb{Z}} \Xi_{d,i}$, where \bigcup stands for the union without repetitions. This subset contains the domain points in all the subintervals induced by the partition of the real line, and it is equal to the subset $\{x_{i+\frac{j}{d}}, i \in \mathbb{Z}\}$, where $x_{i+s} := x_i + s h$ for any irreducible rational number s .

The aim of this paper is to construct quasi-interpolation operators (QIO for short) $\mathcal{Q}_{d,r,k} : C(\mathbb{R}) \rightarrow S_d^r$ exact on \mathbb{P}_k , $k \leq d$, without using a basis of B-splines of S_d^r . This will be achieved by defining the BB-coefficients of the restriction of the quasi-interpolant (QI for short, also for quasi-interpolation) $\mathcal{Q}_{d,r,k} f := \mathcal{Q}_{d,r,k}[f]$ to each subinterval I_i from the values of f at specific points lying in a neighbourhood of I_i depending on the degree (d), the regularity (r) and the exactness (k). As the partition is uniform, it will suffice to define the BB-coefficients associated with the domain points in a set D_i such that $\Xi_d = \bigcup_{i \in \mathbb{Z}} D_i$. A classical result [15] shows that for an enough regular function f there exists a constant C independent of f and h such that $\|\mathcal{Q}_{d,r,k} f - f\|_{\infty, I_i} \leq C h^{k+1} \|f^{(k+1)}\|_{\infty, I_i}$ for all $i \in \mathbb{Z}$.

3. Quadratic quasi-interpolants

This section is devoted to define a QIO $\mathcal{Q}_{2,1,k}$ using the strategy described above.

3.1. QI from point values at knots and midpoints

The C^1 quadratic QI $\mathcal{Q}_{2,1,1} f$ will be constructed assuming that the values $f(x_i)$ and $f(x_{i+\frac{1}{2}})$ are known and such that $\mathcal{Q}_{2,1,1}$ is exact on \mathbb{P}_1 .

Since $\mathcal{Q}_{2,1,1} f \in S_2^1$, following (1) we write

$$\mathcal{Q}f|_{I_i} = \sum_{|\alpha|=2} b_{\alpha,i}(f) \mathfrak{B}_{\alpha,i}.$$

The B-ordinates $b_{\alpha,i}(f)$ are linked to the domain points x_i , $x_{i+\frac{1}{2}}$, and x_{i+1} , so that we choose $D_i = \{x_i, x_{i+\frac{1}{2}}\}$, $i \in \mathbb{Z}$, to produce a partition of Ξ_2 (see Figure 1). Therefore, only $b_{(2,0),i}(f)$ and

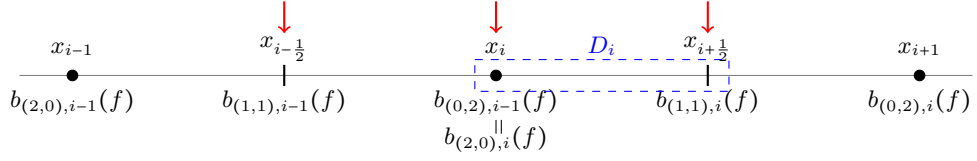


Figure 1: The set D_i , the three points at which the function to be approximated is evaluated and the BB-coefficients involved to get C^1 continuity.

$b_{(1,1),i}(f)$ must be defined so that $\mathcal{Q}_{2,1,1}$ satisfies the required conditions. They will be defined from the values of f at points $\xi_{(1,1),i-1} = x_{i-\frac{1}{2}}$, $\xi_{(2,0),i} = x_i$ and $\xi_{(1,1),i} = x_{i+\frac{1}{2}}$ by writing them in the form

$$b_{\alpha,i}(f) = \mu_{\alpha,0}f\left(x_{i-\frac{1}{2}}\right) + \mu_{\alpha,1}f(x_i) + \mu_{\alpha,2}f\left(x_{i+\frac{1}{2}}\right), \quad \alpha \in \{(2,0), (1,1)\}, \quad (2)$$

so that masks $\mu_\alpha := (\mu_{\alpha,0}, \mu_{\alpha,1}, \mu_{\alpha,2}) \in \mathbb{R}^3$ must be determined.

Proposition 1. *Under the above conditions, the masks $\mu_{(2,0)} = (\frac{1}{2}, 0, \frac{1}{2})$ and $\mu_{(1,1)} = (0, 0, 1)$ are the only ones that give rise to a C^1 quadratic QI $\mathcal{Q}_{2,1,1}f$ such that the operator $\mathcal{Q}_{2,1,1}$ defined as $\mathcal{Q}_{2,1,1}[f] = \mathcal{Q}_{2,1,1}f$ is exact on \mathbb{P}_1 .*

Proof. Let $\mathcal{Q} = \mathcal{Q}_{2,1,1}$. $\mathcal{Q}f$ is C^1 continuous at x_i if and only if

$$b_{(2,0),i}(f) = \frac{1}{2} \left(b_{(1,1),i-1}(f) + b_{(1,1),i}(f) \right).$$

Replacing in this expression each of the BB-coefficients given in (2) and equalling to zero each of their coefficients $f(a + h(i+j))$, the C^1 regularity is equivalent to the following conditions:

$$\mu_{(1,1),0} = \mu_{(1,1),1} = 0, \quad 2\mu_{(2,0),0} = \mu_{(1,1),0} + \mu_{(1,1),2}, \quad 2\mu_{(2,0),1} = \mu_{(1,1),1}, \quad 2\mu_{(2,0),2} = \mu_{(1,1),2}. \quad (3)$$

On the other hand, the exactness of \mathcal{Q} on \mathbb{P}_1 is achieved by imposing that the BB-coefficients of the monomials $m_k(x) := x^k$, $k \in \mathbb{N} \cup \{0\}$, equal those of $\mathcal{Q}m_k$ for $k = 0, 1$. Taking into account that $(1, 1, 1)$ and $(x_i, x_{i+\frac{1}{2}}, x_{i+1})$ are the BB-coefficients relative to I_i of m_0 and m_1 as quadratic polynomials, respectively, and also the expressions of $b_{\alpha,i}(m_k)$ given by (2), after simplification, the required exactness is achieved if and only if the following additional constraints hold:

$$\begin{aligned} \mu_{(2,0),0} + \mu_{(2,0),1} + \mu_{(2,0),2} &= 1, \quad \mu_{(1,1),0} + \mu_{(1,1),1} + \mu_{(1,1),2} = 1, \quad \mu_{(2,0),0} - \mu_{(2,0),2} = 0, \\ -\mu_{(1,1),0} + \mu_{(1,1),2} &= \frac{1}{2}, \quad \mu_{(2,0),0} + 2\mu_{(2,0),1} + 3\mu_{(2,0),2} = 2. \end{aligned} \quad (4)$$

The system constituted by the equations given in (3)-(4) has a unique solution given by the masks appearing in the statement. \square

The BB-coefficients of $\mathcal{Q}_{2,1,1}f$ relative to I_i are

$$b_{(2,0),i}(f) = \frac{1}{2} \left(f\left(x_{i-\frac{1}{2}}\right) + f\left(x_{i+\frac{1}{2}}\right) \right), \quad b_{(1,1),i}(f) = f\left(x_{i+\frac{1}{2}}\right), \quad b_{(0,2),i}(f) = \frac{1}{2} \left(f\left(x_{i+\frac{1}{2}}\right) + f\left(x_{i+\frac{3}{2}}\right) \right).$$

Increasing exactness requires defining the BB-coefficients as linear combinations of five point values $f\left(x_{i-1+\frac{j}{2}}\right)$, $j = 0, 1, 2, 3, 4$ (see Figure 2). Then, we use masks $\mu_\alpha := (\mu_{\alpha,0}, \mu_{\alpha,1}, \mu_{\alpha,2}, \mu_{\alpha,3}, \mu_{\alpha,4})$. In short,

$$b_{\alpha,i}(f) = \sum_{j=0}^4 \mu_{\alpha,j} f\left(x_{i-1+\frac{j}{2}}\right), \quad \alpha \in \{(2,0), (1,1)\}. \quad (5)$$

The following result holds.

Proposition 2. *The masks $\mu_{(2,0)} = (-\frac{1}{4}, 1, -\frac{1}{2}, 1, -\frac{1}{4})$ and $\mu_{(1,1)} = (0, 0, -\frac{1}{2}, 2, -\frac{1}{2})$ produce the unique C^1 quadratic QI $\mathcal{Q}_{2,1,2}f$ such that the operator $\mathcal{Q}_{2,1,2}$ defined as $\mathcal{Q}_{2,1,2}[f] = \mathcal{Q}_{2,1,2}f$ is exact on \mathbb{P}_2 .*

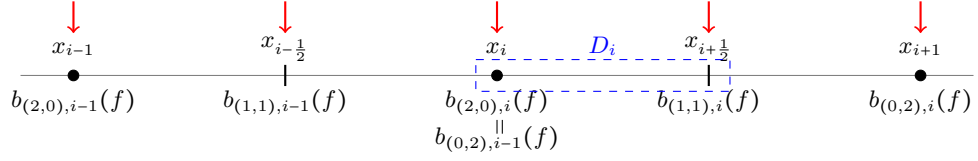


Figure 2: The set D_i , the five knots and midpoints around x_i at which the function to be approximated is evaluated, and the BB-coefficients involved to get C^1 continuity.

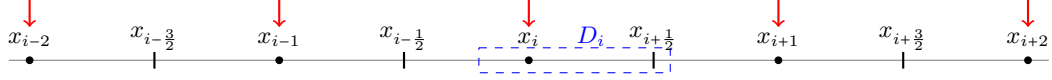


Figure 3: The set D_i , the five knots around x_i at which the function to be approximated is evaluated, and the BB-coefficients involved to get C^1 continuity.

Proof. The proof runs as in Proposition 1. By (5), $\mathcal{Q} = \mathcal{Q}_{2,1,2}$ is C^1 continuous at x_i if and only if $\mu_{(1,1),0} = \mu_{(1,1),1} = 0$ and

$$\begin{aligned} 2\mu_{(2,0),0} - \mu_{(1,1),0} - \mu_{(1,1),2} &= 0, & 2\mu_{(2,0),1} - \mu_{(1,1),1} - \mu_{(1,1),3} &= 0, & 2\mu_{(2,0),2} - \mu_{(1,1),2} - \mu_{(1,1),4} &= 0, \\ 2\mu_{(2,0),3} - \mu_{(1,1),3} &= 0, & 2\mu_{(2,0),4} - \mu_{(1,1),4} &= 0. \end{aligned}$$

The exactness of \mathcal{Q} on \mathbb{P}_2 is equivalent to the following conditions:

$$\begin{aligned} \mu_{(2,0),0} + \mu_{(2,0),1} + \mu_{(2,0),2} + \mu_{(2,0),3} + \mu_{(2,0),4} &= 1, & \mu_{(1,1),0} + \mu_{(1,1),1} + \mu_{(1,1),2} + \mu_{(1,1),3} + \mu_{(1,1),4} &= 1, \\ \mu_{(2,0),0} + \frac{1}{2}\mu_{(2,0),1} - \frac{1}{2}\mu_{(2,0),3} - \mu_{(2,0),4} &= 0, & \mu_{(1,1),0} + \frac{1}{2}\mu_{(1,1),1} - \frac{1}{2}\mu_{(1,1),3} - \mu_{(1,1),4} &= \frac{1}{2}, \\ \frac{1}{2}\mu_{(2,0),1} + \mu_{(2,0),2} + \frac{3}{2}\mu_{(2,0),3} + 2\mu_{(2,0),4} &= 1, & \mu_{(2,0),0} + \frac{1}{4}\mu_{(2,0),1} + \frac{1}{4}\mu_{(2,0),3} + \mu_{(2,0),4} &= 0, \\ \mu_{(1,1),0} + \frac{1}{4}\mu_{(1,1),1} + \frac{1}{4}\mu_{(1,1),3} + \mu_{(1,1),4} &= 0, & \frac{1}{4}\mu_{(2,0),1} + \mu_{(2,0),2} + \frac{9}{2}\mu_{(2,0),3} + 4\mu_{(2,0),4} &= 1. \end{aligned}$$

Solving the system with these 15 linear equations the claim follows. \square

The obtained masks determine the QI $\mathcal{Q}_{2,1,2}f$ in each interval: its BB-coefficients are

$$\begin{aligned} b_{(2,0),i}(f) &= -\frac{1}{4}f(x_{i-1}) + f(x_{i-1/2}) - \frac{1}{2}f(x_i) + f(x_{i+1/2}) - \frac{1}{4}f(x_{i+1}), \\ b_{(1,1),i}(f) &= -\frac{1}{2}f(x_i) + 2f(x_{i+1/2}) - \frac{1}{2}f(x_{i+1}), \\ b_{(0,2),i}(f) &= -\frac{1}{4}f(x_i) + f(x_{i+1/2}) - \frac{1}{2}f(x_{i+1}) + f(x_{i+3/2}) - \frac{1}{4}f(x_{i+2}). \end{aligned}$$

3.2. QI from point values at knots

We complete the quadratic case by considering the construction of QIs $\mathcal{Q}_{2,1,2}^{\text{kn}}f$ exact on \mathbb{P}_2 assuming that only the values of the knots are known (see Figure 3), i.e., we consider BB-coefficients of the form

$$b_{\alpha,i}(f) = \sum_{j=0}^4 \mu_{\alpha,j} f(x_{i+j-2}), \quad \alpha \in \{(2,0), (1,1)\}. \quad (6)$$

The superscript kn is used to indicate that the QI is defined only from point values at knots.

Proposition 3. *Let us suppose that the BB-coefficients of $\mathcal{Q}_{2,1,2}^{\text{kn}}f$ relative to the interval I_i are given by (6). Then, the operator $\mathcal{Q}_{2,1,2}^{\text{kn}}$ defined as $\mathcal{Q}_{2,1,2}^{\text{kn}}[f] = \mathcal{Q}_{2,1,2}^{\text{kn}}f$ is exact on \mathbb{P}_2 and produces C^1 QIs if and only if $\mu_{(2,0)} = (\lambda, \frac{1}{8} - 2\lambda, \frac{5}{8}, \frac{3}{8} + 2\lambda, -\frac{1}{8} - \lambda)$ and $\mu_{(1,1)} = (0, 2\lambda, \frac{1}{4} - 6\lambda, 1 + 6\lambda, -\frac{1}{4} - 2\lambda)$ with $\lambda \in \mathbb{R}$.*

Proof. The proof is similar to those of Propositions 1 and 2. With the masks given in (5), $\mathcal{Q}f = \mathcal{Q}_{2,1,2}^{\text{kn}} f$ is C^1 continuous at x_i if and only if $\mu_{(1,1),0} = 0$, $-2\mu_{(2,0),4} + \mu_{(1,1),4} = 0$ and

$$-2\mu_{(2,0),k} + \mu_{(1,1),k} + \mu_{(1,1),k+1} = 0, \quad k = 0, 1, 2, 3.$$

The exactness of \mathcal{Q} on \mathbb{P}_2 is equivalent to the following conditions:

$$\begin{aligned} \mu_{(2,0),0} + \mu_{(2,0),1} + \mu_{(2,0),2} + \mu_{(2,0),3} + \mu_{(2,0),4} &= 1, & \mu_{(1,1),0} + \mu_{(1,1),1} + \mu_{(1,1),2} + \mu_{(1,1),3} + \mu_{(1,1),4} &= 1, \\ -2\mu_{(2,0),0} - \mu_{(2,0),1} + \mu_{(2,0),3} + 2\mu_{(2,0),4} &= 0, & -2\mu_{(1,1),0} - \mu_{(1,1),1} + \mu_{(1,1),3} + 2\mu_{(1,1),4} &= \frac{1}{2}, \\ -\mu_{(2,0),0} + \mu_{(2,0),2} + 2\mu_{(2,0),3} + 3\mu_{(2,0),4} &= 1, & 4\mu_{(1,1),0} + \mu_{(1,1),1} + \mu_{(1,1),3} + 4\mu_{(1,1),4} &= 0, \\ \mu_{(2,0),0} + \mu_{(2,0),2} + 4\mu_{(2,0),3} + 9\mu_{(2,0),4} &= 1, & 4\mu_{(2,0),0} + \mu_{(2,0),1} + \mu_{(2,0),3} + 4\mu_{(2,0),4} &= 0. \end{aligned}$$

The solution of this system leads to the masks in the statement. \square

The obtained masks determine $\mathcal{Q}_{2,1,2}^{\text{kn}} f$ in each interval I_i : its BB-coefficients are

$$\begin{aligned} b_{(2,0),i}(f) &= \lambda f(x_{i-2}) + \left(\frac{1}{8} - 2\lambda\right) f(x_{i-1}) + \frac{5}{8} f(x_i) + \left(\frac{3}{8} + 2\lambda\right) f(x_{i+1}) - \left(\frac{1}{8} + \lambda\right) f(x_{i+2}), \\ b_{(1,1),i}(f) &= 2\lambda f(x_{i-1}) + \left(\frac{1}{4} - 6\lambda\right) f(x_i) + (1 + 6\lambda) f(x_{i+1}) - \left(\frac{1}{4} + 2\lambda\right) f(x_{i+2}), \\ b_{(0,2),i}(f) &= \lambda f(x_{i-1}) + \left(\frac{1}{8} - 2\lambda\right) f(x_i) + \frac{5}{8} f(x_{i+1}) + \left(\frac{3}{8} + 2\lambda\right) f(x_{i+2}) - \left(\frac{1}{8} + \lambda\right) f(x_{i+3}). \end{aligned}$$

Remark 1. It might be thought that this constructive process would lead to the same masks as those provided by the classical QI exact on \mathbb{P}_2 based on the C^1 quadratic B-spline M_3 centered at the origin (see [16]), i.e.

$$\mathcal{Q}f = \sum_{i \in \mathbb{Z}} \frac{1}{8} (-f(a + h(i-1)) + 10f(a + hi) - f(a + h(i+1))) M_3\left(\frac{\cdot - a}{h} - i\right).$$

They are $(-\frac{1}{16}, \frac{9}{16}, \frac{9}{16}, -\frac{1}{16}, 0)$ and $(0, -\frac{1}{8}, \frac{5}{4}, -\frac{1}{8}, 0)$. It is clear that no value of λ leads to these masks.

Remark 2. Having a free parameter would allow the construction of QIs with particular characteristics, such as superconvergence at specific points, typically the knots and midpoints of the I_i intervals. A simple calculation proves that $\lambda = -\frac{1}{16}$ produces errors

$$\begin{aligned} \left| \mathcal{Q}_{2,1,2}^{\text{kn}} f(x_i) - f(x_i) \right| &= \left| b_{(2,0),i}(f) - f(x_i) \right| = \mathcal{O}(h^4), \\ \left| \mathcal{Q}_{2,1,2}^{\text{kn}} f\left(x_i + \frac{h}{2}\right) - f\left(x_i + \frac{h}{2}\right) \right| &= \left| \frac{1}{4} (b_{(2,0),i}(f) + 2b_{(1,1),i}(f) + b_{(2,0),i+1}(f)) - f\left(x_i + \frac{h}{2}\right) \right| = \mathcal{O}(h^4). \end{aligned}$$

The resulting masks are

$$\mu_{(2,0)} = \left(-\frac{1}{16}, \frac{1}{4}, \frac{5}{8}, \frac{1}{4}, -\frac{1}{16}\right) \quad \text{and} \quad \mu_{(1,1)} = \left(0, -\frac{1}{8}, \frac{5}{8}, \frac{5}{8}, -\frac{1}{8}\right).$$

Consider the differential QI

$$Df = \sum_{i \in \mathbb{Z}} \left(f\left(x_{i-\frac{1}{2}}\right) - \frac{h^2}{8} f''\left(x_{i-\frac{1}{2}}\right) \right) M_i,$$

where M_i is the quadratic B-spline supported on $[a + (j-2)h, a + (j+1)h]$. It is exact on \mathbb{P}_2 .

If the linear functional

$$d_i[f] := f\left(x_{i-\frac{1}{2}}\right) - \frac{h^2}{8} f''\left(x_{i-\frac{1}{2}}\right)$$

is discretized from the values of f at the knots lying in the support of M_i , then the linear functional

$$\tilde{d}_i[f] := \frac{1}{8} (-f(x_{i-2}) + 5f(x_{i-1}) + 5f(x_i) - f(x_{i+1}))$$

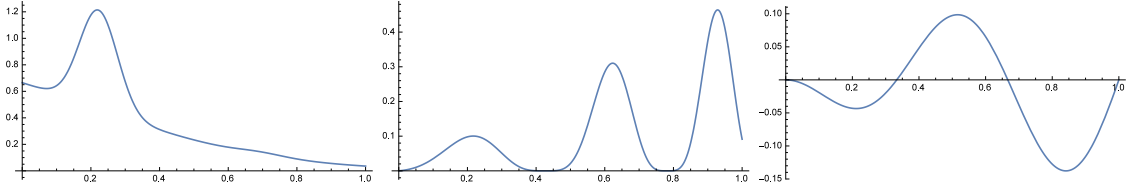


Figure 4: From left to right, the plots of test functions f_1 , f_2 and f_3 .

results. The masks corresponding to

$$\tilde{D}f = \sum_{i \in \mathbb{Z}} \tilde{d}_i[f] M_i$$

are also $\mu_{(2,0)}$ and $\mu_{(1,1)}$.

Remark 3. Another way to choose a value of the parameter λ is to minimize an upper bound of the infinity norm of the operator $\mathcal{Q}_{2,1,2}^{kn}$. Since

$$\|\mathcal{Q}_{2,1,2}^{kn}\|_{\infty} \leq \max\{\|\mu_{(2,0)}\|_1, \|\mu_{(1,1)}\|_1\},$$

where the 1-norm of $v := (v_1, \dots, v_n)$ is given by $\|v\|_1 := \sum_{i=1}^n |v_i|$, we propose to determine λ by minimizing

$$\begin{aligned} U_2(\lambda) &:= \max\{\|\mu_{(2,0)}\|_1, \|\mu_{(1,1)}\|_1\} \\ &= \max\left\{\frac{5}{8} + \left|\frac{1}{8} - 2\lambda\right| + \left|\frac{1}{8} + \lambda\right| + |\lambda| + \left|\frac{3}{8} + 2\lambda\right|, \left|\frac{1}{4} - 6\lambda\right| + \left|\frac{1}{4} + 2\lambda\right| + 2|\lambda| + |1 + 6\lambda|\right\}. \end{aligned}$$

This is a (non strictly) convex function. Its absolute minimum is equal to $\frac{3}{2}$. It is attained at every value of λ lying in the interval $[-\frac{1}{8}, 0]$. The value $\lambda = 0$ produces the masks $\mu_{(2,0)} = (0, \frac{1}{8}, \frac{5}{8}, \frac{3}{8}, -\frac{1}{8})$ and $\mu_{(1,1)} = (0, 0, \frac{1}{4}, 1, -\frac{1}{4})$. And $\lambda = -\frac{1}{8}$ gives the masks $\mu_{(2,0)} = (-\frac{1}{8}, \frac{3}{8}, \frac{5}{8}, \frac{1}{8}, 0)$ and $\mu_{(1,1)} = (0, -\frac{1}{4}, 1, \frac{1}{4}, 0)$.

3.3. Numerical tests

To test the performance of some of the obtained C^1 quadratic QIs we will use the following functions:

$$\begin{aligned} f_1(x) &= \frac{3}{4}e^{-2(9x-2)^2} - \frac{1}{5}e^{-(9x-7)^2 - (9x-4)^2} + \frac{1}{2}e^{-(9x-7)^2 - \frac{1}{4}(9x-3)^2} + \frac{3}{4}e^{\frac{1}{10}(-9x-1) - \frac{1}{49}(9x+1)^2}, \\ f_2(x) &= \frac{1}{2}x \cos^4(4(x^2 + x - 1)), \\ f_3(x) &= -\frac{1}{4}xe^{-x/2} \sin(3\pi x). \end{aligned}$$

Functions f_1 and f_2 are the 1D-versions of Franke's and Nielson's functions [17, 18]. Their plots over the interval $I = [0, 1]$ appear in Figure 4, and their QIs will be defined in I . The tests are carried out for a sequence of uniform mesh with knots $x_i = ih$, $i = 0, \dots, n$, where $h = \frac{1}{n}$.

In general, for a given QI $\mathcal{Q}_n f$, the associated error is estimated as

$$\mathcal{E}_n(f) = \max_{0 \leq \ell \leq 200} |\mathcal{Q}_n f(z_\ell) - f(z_\ell)|,$$

where z_ℓ are equally spaced points in I . The estimated numerical convergence order (NCO) is given by the rate

$$NCO := \frac{\log(\mathcal{E}_{n_1}/\mathcal{E}_{n_2})}{\log(n_2/n_1)}.$$

Table 1 shows the errors and NCOs obtained for the three test functions using the two considered from the QIs given in Proposition 2 and Remark 2. They are in good agreement with the theoretical results.

Figure 5 shows the plots of the errors incurred when approximating the test functions in the interval I by the QIs whose masks are given in Proposition 2 and Remark 2. Visually the graphs of the QIs are indistinguishable from those of the test functions. The results provided by the QI based on values at knots and midpoints are slightly better.

n	f_1		f_2		f_3	
	error	NCO	error	NCO	error	NCO
16	2.58×10^{-2}		5.67×10^{-2}		3.59×10^{-4}	
32	3.31×10^{-3}	2.964	4.63×10^{-3}	3.618	3.47×10^{-5}	3.373
64	2.56×10^{-4}	3.692	3.49×10^{-4}	3.729	3.88×10^{-6}	3.159
128	2.48×10^{-5}	3.368	3.36×10^{-5}	3.380	4.68×10^{-7}	3.052
256	2.96×10^{-6}	3.068	3.60×10^{-6}	3.220	5.77×10^{-8}	3.019
n	error	NCO	error	NCO	error	NCO
16	7.62×10^{-2}		9.58×10^{-2}		1.10×10^{-3}	
32	1.08×10^{-2}	2.822	1.40×10^{-2}	2.772	7.60×10^{-5}	3.853
64	8.17×10^{-4}	3.722	1.13×10^{-3}	3.639	5.93×10^{-6}	3.679
128	5.56×10^{-5}	3.877	7.85×10^{-5}	3.842	5.60×10^{-7}	3.404
256	4.13×10^{-6}	3.752	6.15×10^{-6}	3.674	6.33×10^{-8}	3.146

Table 1: Errors and NCOs for f_1 , f_2 and f_3 in applying the QIs in Proposition 2 (top) and Remark 2.

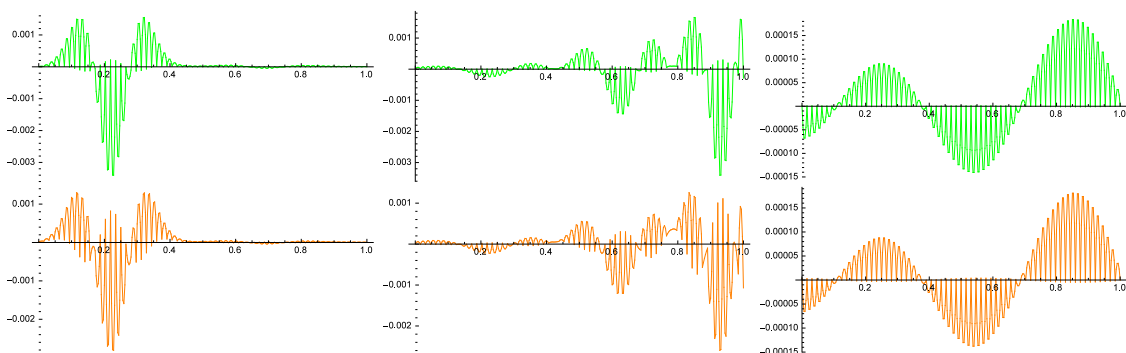


Figure 5: Plots of QI errors for f_1 , f_2 and f_3 after dividing the interval I into $n = 64$ equal parts. Top, those corresponding to C^1 quadratic QI exact on \mathbb{P}_2 based on values at knots and midpoints. Bottom, those provided by $\mathcal{Q}_{2,1,2}^{\text{kn}}$ with $\lambda = -\frac{1}{16}$.

4. Cubic quasi-interpolants

This section aims to construct cubic QIs $\mathcal{Q}_{3,r,k}$ following a procedure similar to the one used above. Although the exactness on \mathbb{P}_1 and \mathbb{P}_2 could be imposed, we will restrict ourselves to the case $k = 3$ to define operators $\mathcal{Q}_{3,r} := \mathcal{Q}_{3,r,3}$. The first step is to choose a partition of Ξ_3 . This case allows to select a subset symmetrical with respect to the knot, namely $D_i = \left\{x_{i-\frac{1}{3}}, x_i, x_{i+\frac{1}{3}}\right\}$, so that only the BB-coefficients associated with those domain points have to be defined. We write

$$\mathcal{Q}_{3,r}f|_{I_i} = \sum_{|\alpha|=3} b_{\alpha,i}(f) \mathfrak{B}_{\alpha,i},$$

and we opt to simplify the notation by not indicating that the BB-coefficients $b_{\alpha,i}(f)$ depend on r .

4.1. C^1 cubic quasi-interpolation from point values at knots and midpoints

Also in this case we guess

$$b_{\alpha,i}(f) = \sum_{j=0}^4 \mu_{\alpha,j} f\left(x_{i-1+\frac{j}{2}}\right), \quad \alpha \in \{(3,0), (2,1), (1,2)\}, \quad (7)$$

for masks $\mu_\alpha := (\mu_{\alpha,0}, \mu_{\alpha,1}, \mu_{\alpha,2}, \mu_{\alpha,3}, \mu_{\alpha,4})$. Figure 6 shows how the subset D_i is chosen, as well as the points at which the function is evaluated to define the BB-coefficients.

We have the following result.

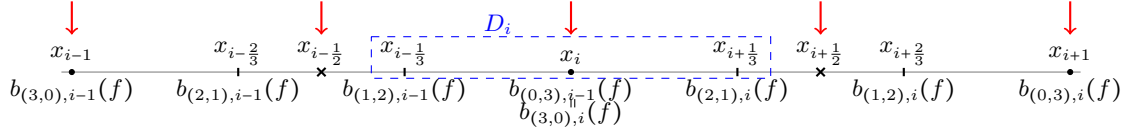


Figure 6: The BB-coefficients associated with the three points in the set D_i are calculated from point values at the five marked knots and midpoints.

Proposition 4. *The operator $\mathcal{Q}_{3,1}$ is exact on \mathbb{P}_3 and produces C^1 cubic QIs if and only if*

$$\begin{aligned}\mu_{(3,0)} &= (\kappa, -4\kappa, 1 + 6\kappa, -4\kappa, \kappa), \\ \mu_{(2,1)} &= \left(-\frac{1}{18} + \frac{1}{4}\lambda + 2\kappa, -\lambda - 8\kappa, \frac{1}{3} + \frac{3}{2}\lambda + 12\kappa, \frac{8}{9} - \lambda - 8\kappa, -\frac{1}{6} + \frac{1}{4}\lambda + 2\kappa\right), \\ \mu_{(1,2)} &= \left(\frac{1}{36}(2 - 9\lambda), \lambda, \frac{1}{6}(10 - 9\lambda), \frac{1}{9}(9\lambda - 8), \frac{1}{12}(2 - 3\lambda)\right),\end{aligned}$$

with $\kappa, \lambda \in \mathbb{R}$.

Proof. The proof is similar to that of Proposition 1. $\mathcal{Q}_{3,1}f$ is C^1 -continuous at x_i if and only if

$$b_{(3,0),i}(f) = \frac{1}{2} \left(b_{(1,2),i-1}(f) + b_{(2,1),i}(f) \right).$$

This, together with conditions equivalent to the exactness on \mathbb{P}_3 , results in a system on 20 equations, having the 2-parametric family of solutions given in the statement. \square

The parameters can be chosen to satisfy various properties of interest, as in Section 3. For example, the QI could interpolate the point values at the knots, or be superconvergent at certain points, or be near-minimally normed, or a combination of properties, if compatible. In the following we indicate the conditions on the parameters leading to the considered properties.

INTERPOLATION AT KNOTS

Since $\mu_{(3,0)} = (\kappa, -4\kappa, 1 + 6\kappa, -4\kappa, \kappa)$, the value $\kappa = 0$ produces the mask $(0, 0, 1, 0, 0)$ for the BB-coefficient $b_{(3,0),i}(f)$, so it is equal to $f(x_i)$ and the QI interpolates the value of f at x_i . The parameter λ remains free, so interpolation at knots can be combined with the minimization of an upper bound of the infinity norm of the resulting operator, $\mathcal{Q}_{3,1}^0$, defined from the masks $\mu_{(3,0)}^0 = (0, 0, 1, 0, 0)$, $\mu_{(2,1)}^0 = \left(-\frac{1}{18} + \frac{1}{4}\lambda, -\lambda, \frac{1}{3} + \frac{3}{2}\lambda, \frac{8}{9} - \lambda, -\frac{1}{6} + \frac{1}{4}\lambda\right)$ and

$$\mu_{(1,2)}^0 = \left(\frac{1}{36}(2 - 9\lambda), \lambda, \frac{1}{6}(10 - 9\lambda), \frac{1}{9}(-8 + 9\lambda), \frac{1}{12}(2 - 3\lambda)\right).$$

Therefore, an upper bound to $\|\mathcal{Q}_{3,1}^0\|_\infty$ is given by

$$\begin{aligned}U_3^0(\lambda) &:= \max \left\{ \|\mu_{(3,0)}^0\|_1, \|\mu_{(2,1)}^0\|_1, \|\mu_{(1,2)}^0\|_1 \right\} \\ &= \max \left\{ 1, \frac{1}{36}|2 - 9\lambda| + |\lambda| + \frac{1}{6}|2 + 9\lambda| + \frac{1}{9}|8 - 9\lambda| + \frac{1}{12}|2 - 3\lambda|, \right. \\ &\quad \left. \frac{1}{36}|2 - 9\lambda| + |\lambda| + \frac{1}{6}|10 - 9\lambda| + \frac{1}{9}|8 - 9\lambda| + \frac{1}{12}|2 - 3\lambda| \right\}.\end{aligned}$$

It is a strictly convex function (see Figure 7). It reaches its absolute minimum only at $\lambda = \frac{4}{9}$, providing the QIO $\mathcal{Q}_{3,1}^{0,\frac{4}{9}}$ defined from $(0, 0, 1, 0, 0)$, $\left(\frac{1}{18}, -\frac{4}{9}, 1, \frac{4}{9}, -\frac{1}{18}\right)$ and $\left(-\frac{1}{18}, \frac{4}{9}, 1, -\frac{4}{9}, \frac{1}{18}\right)$.

Table 2 shows the errors and NCOs when $\mathcal{Q}_{3,1}^{0,\frac{4}{9}}$ is applied to approximate f_1 , f_2 and f_3 . It uses point values at knots and midpoints and is interpolatory at knots.

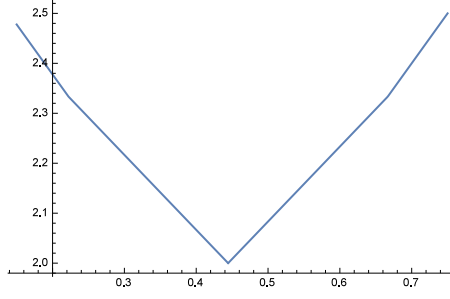


Figure 7: Graph of the objective function U_3^0 in a neighbourhood of the point at which it attains its minimum value.

n	f_1		f_2		f_3	
	error	NCO	error	NCO	error	NCO
16	1.15×10^{-2}		8.43×10^{-3}		4.85×10^{-5}	
32	5.67×10^{-4}	4.346	7.81×10^{-4}	3.432	3.02×10^{-6}	4.007
64	3.72×10^{-5}	3.929	5.14×10^{-5}	3.925	1.87×10^{-7}	4.015
128	2.17×10^{-6}	4.098	3.16×10^{-6}	4.025	1.18×10^{-8}	3.990
256	1.39×10^{-7}	3.968	1.80×10^{-7}	4.133	7.18×10^{-10}	4.034

Table 2: Errors and NCOs obtained when $\mathcal{Q}_{3,1}^{0, \frac{4}{9}}$ is used for approximating f_1 , f_2 and f_3 .

SUPERCONVERGENCE AT MIDPOINTS

Applying de Casteljaeu's algorithm, the value of $\mathcal{Q}_{3,1}$ at midpoint $x_{i+\frac{1}{2}}$ is given by the expression

$$q_{1/2}(f) := \frac{1}{8} (b_{(3,0),i}(f) + 3b_{(2,1),i}(f) + 3b_{(1,2),i+1}(f) + b_{(3,0),i+1}(f)).$$

As the operator is exact on \mathbb{P}_3 , the error $\varepsilon_{1/2}(f) := q_{1/2}(f) - f(x_{i+\frac{1}{2}})$ is null on \mathbb{P}_3 . A simple calculation shows that $\varepsilon_{1/2}(m_4) = \frac{1}{16}h^4(-1 + 24\kappa)$. Therefore, the choice $\kappa = 1/24$ gives rise to a QI $\mathcal{Q}_{3,1}^{\frac{1}{24}}f$ superconvergent at $x_{i+\frac{1}{2}}$. As again λ is a free parameter, so it is also possible to minimize the infinity norm to $\mathcal{Q}_{3,1}^{\frac{1}{24}}$. In this case, the minimum value of the upper bound is reached uniquely at $\lambda = \frac{5}{18}$, which provides for $\mathcal{Q}_{3,1}^{\frac{1}{24}, \frac{5}{18}}$ the masks $\mu_{(3,0)} = (\frac{1}{24}, -\frac{1}{6}, \frac{5}{4}, -\frac{1}{6}, \frac{1}{24})$, $\mu_{(2,1)} = (\frac{7}{72}, -\frac{11}{18}, \frac{5}{4}, \frac{5}{18}, -\frac{1}{72})$ and $\mu_{(1,2)} = (-\frac{1}{72}, \frac{5}{18}, \frac{5}{4}, -\frac{11}{18}, \frac{7}{72})$.

SUPERCONVERGENCE AT DOMAIN POINTS INSIDE INTERVALS

Analogously, given that the values of $\mathcal{Q}_{3,1}$ at $x_{i+\frac{1}{3}}$ and $x_{i+\frac{2}{3}}$ are

$$q_{1/3}(f) := \frac{1}{27} (8b_{(3,0),i}(f) + 12b_{(2,1),i}(f) + 6b_{(1,2),i+1}(f) + b_{(3,0),i+1}(f))$$

and

$$q_{2/3}(f) := \frac{1}{27} (b_{(3,0),i}(f) + 6b_{(2,1),i}(f) + 12b_{(1,2),i+1}(f) + 8b_{(3,0),i+1}(f)),$$

respectively, the errors $\varepsilon_{1/3}(f) := q_{1/3}(f) - f(x_{i+\frac{1}{3}})$ and $\varepsilon_{2/3}(f) := q_{2/3}(f) - f(x_{i+\frac{2}{3}})$ are null on \mathbb{P}_3 and the equalities $\varepsilon_{2/3}(m_4) = \frac{h^4}{324}(27\lambda + 594\kappa - 28)$ and $\varepsilon_{1/3}(m_4) = \frac{h^4}{324}(27\lambda - 378\kappa + 4)$ hold. Therefore, superconvergence is achieved at $x_i + \frac{h}{3}$ if $27\lambda + 594\mu = 28$, while it will be realised at $x_i + \frac{2h}{3}$ if $27\lambda - 378\mu = -4$. It is obtained at both points if and only if $\kappa = 8/243$ and $\lambda = 76/243$, in which case the masks are $\mu_{(3,0)} = (\frac{8}{243}, -\frac{32}{243}, \frac{97}{81}, -\frac{32}{243}, \frac{8}{243})$, $\mu_{(2,1)} = (\frac{43}{486}, -\frac{140}{243}, \frac{97}{81}, \frac{76}{243}, -\frac{11}{486})$ and $\mu_{(1,2)} = (-\frac{11}{486}, \frac{76}{243}, \frac{97}{81}, -\frac{140}{243}, \frac{43}{486})$. They provide the QIO $\mathcal{Q}_{3,1}^{\frac{8}{243}, \frac{76}{243}}$.

For this operator Table 3 shows the errors and NCOs when the tests functions are approximated. Plots of QI errors for $n = 64$ appear in Figure 8.

n	f_1		f_2		f_3	
	error	NCO	error	NCO	error	NCO
16	9.25×10^{-3}		7.45×10^{-3}		3.68×10^{-5}	
32	4.13×10^{-4}	4.485	5.70×10^{-4}	3.707	2.31×10^{-6}	3.994
64	2.48×10^{-5}	4.057	3.79×10^{-5}	3.910	1.44×10^{-7}	4.006
128	1.77×10^{-6}	3.809	2.41×10^{-6}	3.974	8.62×10^{-9}	4.060
256	1.10×10^{-7}	4.010	1.52×10^{-7}	3.993	5.79×10^{-10}	3.898

Table 3: Errors $\left| f_\ell - \mathcal{Q}_{3,1}^{\frac{8}{243}, \frac{76}{243}} f_\ell \right|$, $\ell = 1, 2, 3$, and NCOs.

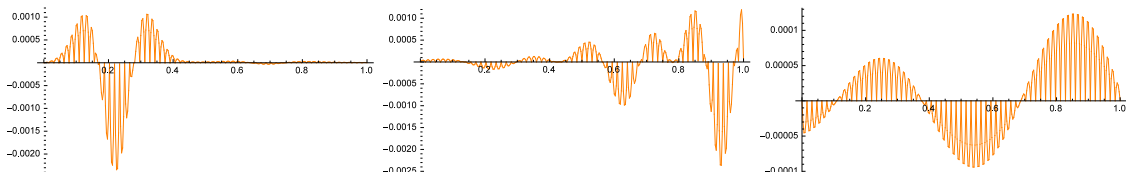


Figure 8: Plots of QI errors when the operator $\mathcal{Q}_{3,1}^{\frac{8}{243}, \frac{76}{243}}$ is applied to f_ℓ , $\ell = 1, 2, 3$

SMALL INFINITY NORM

Another way to select the parameters λ and μ is to minimize the upper bound

$$\begin{aligned}
U_3(\lambda, \mu) &:= \max \left\{ \|\mu_{(3,0)}\|_1, \|\mu_{(2,1)}\|_1, \|\mu_{(1,2)}\|_1 \right\} \\
&= \frac{1}{36} \max \left\{ |2 - 9\lambda| + 4|8 - 9\lambda| + 6|10 - 9\lambda| + 3|2 - 3\lambda| + 36|\lambda|, 10|\kappa| + |1 + 6\kappa|, \right. \\
&\quad \left. 4|9\lambda + 72\kappa - 8| + 36|\lambda + 8\kappa| + 3|3\lambda + 24\kappa - 2| + |9\lambda + 72\kappa - 2| + 6|9\lambda + 72\kappa| + 2 \right\}
\end{aligned}$$

of the infinity norm of $\mathcal{Q}_{3,1}$. It is a strictly convex function and Figure 9 shows the structure of the projection of the graph of U_3 around the unique point where it reaches its absolute minimum: it is the point of intersection of four planes. It follows that $\|\mathcal{Q}_{3,1}\|_\infty \leq U_3\left(\frac{8}{9}, -\frac{1}{9}\right) = \frac{13}{9}$. The masks associated with these parameter values are $\mu_{(3,0)} = \left(-\frac{1}{9}, \frac{4}{9}, \frac{1}{3}, \frac{4}{9} - \frac{1}{9}\right)$, $\mu_{(2,1)} = \left(-\frac{1}{18}, 0, \frac{1}{3}, \frac{8}{9}, -\frac{1}{6}\right)$ and $\mu_{(1,2)} = \left(-\frac{1}{6}, \frac{8}{9}, \frac{1}{3}, 0, -\frac{1}{18}\right)$.

4.2. C^1 quasi-interpolation from point values at knots

When only the point values at knots are known, we look for a QIO $\mathcal{Q}_{3,1}^{\text{kn}}$ exact on \mathbb{P}_3 such that $\mathcal{Q}_{3,1}^{\text{kn}} f$ is C^1 continuous. Its BB-coefficients are of the form

$$b_{\alpha,i}(f) = \sum_{j=0}^4 \mu_{\alpha,j} f(x_{i-2+j}), \quad \alpha \in \{(3,0), (2,1), (1,2)\} \quad (8)$$

for masks $\mu_\alpha := (\mu_{\alpha,0}, \mu_{\alpha,1}, \mu_{\alpha,2}, \mu_{\alpha,3}, \mu_{\alpha,4})$ (see Figure 10).

The following result holds, whose proof goes as in the previous cases.

Proposition 5. *The operator $\mathcal{Q}_{3,1}^{\text{kn}}$ is exact on \mathbb{P}_3 and produces C^1 cubic QI if and only if*

$$\begin{aligned}
\mu_{(3,0)} &= (\kappa, -4\kappa, 1 + 6\kappa, -4\kappa, \kappa), \\
\mu_{(2,1)} &= \left(-\lambda + 2\kappa, -\frac{1}{9} + 4\lambda - 8\kappa, \frac{5}{6} - 6\lambda + 12\kappa, \frac{1}{3} + 4\lambda - 8\kappa, -\frac{1}{18} - \lambda + 2\kappa\right), \\
\mu_{(1,2)} &= \left(\lambda, \frac{1}{9} - 4\lambda, \frac{7}{6} + 6\lambda, -\frac{1}{3} - 4\lambda, \frac{1}{18} + \lambda\right),
\end{aligned}$$

κ and λ being free parameters.

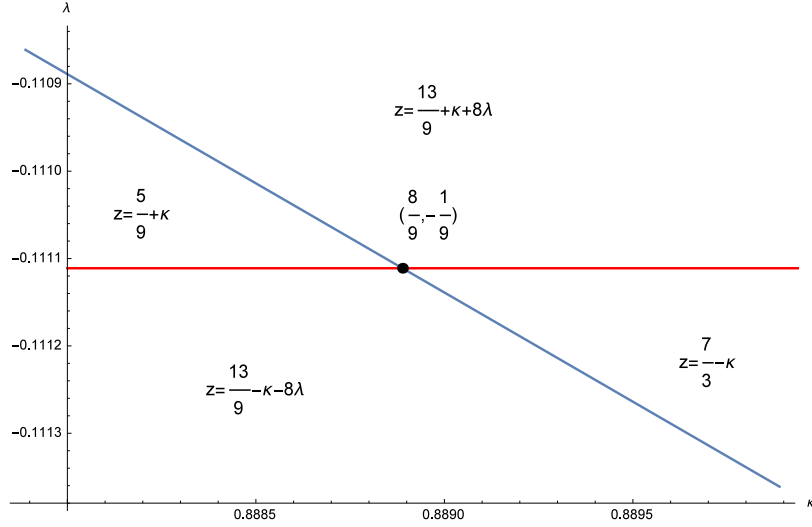


Figure 9: Projection of the graph of the objective function in a neighbourhood of the point at which its absolute minimum is attained.

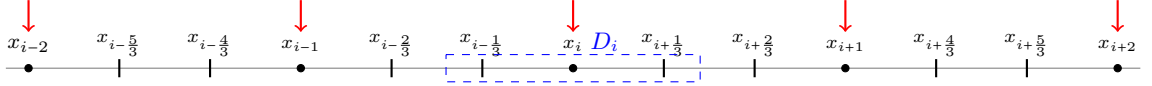


Figure 10: The BB-coefficients associated with the three points in the set D_i are calculated from point values at the five marked knots.

Again, the two-parameter dependence allows one to construct QIs with specific properties: interpolation (I), superconvergence at the midpoints (SC 1/2), superconvergence at a point resulting from dividing each interval into three equal parts (SC 1/3 & SC 2/3), or minimum value of the upper bound of the uniform norm of the operator provided by the maximum of the 1-norm of the masks, i.e. near-best (NB-) QI.

Table 4 shows the results obtained in several cases combining superconvergence, interpolation and near minimal infinity norm.

As shown in Table 4, when interpolation is required at the knots, the parameter κ takes the value zero and λ is free. This allows to minimize the upper bound of the uniform norm of the operator provided by the 1-norms of the masks. It is a strictly convex function, whose absolute minimum is reached at $\lambda = -\frac{1}{36}$. Therefore, for $\kappa = 0$ and $\lambda = -\frac{1}{36}$ the uniform norm of the QIO is less than or equal to $3/2$ and the masks associated with x_i , $x_i + \frac{h}{3}$ and $x_i - \frac{h}{3}$ are $(0, 0, 1, 0, 0)$, $(\frac{1}{36}, -\frac{2}{9}, 1, \frac{2}{9}, -\frac{1}{36})$ and $(-\frac{1}{36}, \frac{2}{9}, 1, -\frac{2}{9}, \frac{1}{36})$, respectively.

Also the SC 1/2 case shown in Table 4 ($\kappa = \frac{1}{384}$) gives rise to a family of masks depending on λ . Again, it is possible to determine its value in such a way that it results in an operator with almost minimal infinity norm. It is straightforward to prove that the upper bound attains at $\lambda = -\frac{29}{1152}$ its minimum value, which is equal to $\frac{97}{64} \approx 1.516$. The masks of x_i , $x_i + \frac{h}{3}$ and $x_i - \frac{h}{3}$ are $(\frac{1}{384}, -\frac{1}{96}, \frac{65}{64}, -\frac{1}{96}, \frac{1}{384})$, $(\frac{35}{1152}, -\frac{67}{288}, \frac{65}{64}, \frac{61}{288}, -\frac{29}{1152})$ and $(-\frac{29}{1152}, \frac{61}{288}, \frac{65}{64}, -\frac{67}{288}, \frac{13}{1152})$, respectively.

Regarding the result on the NB case included in Table 4, Figure 11 illustrates the structure of the objective function near the (unique) point where it attains its absolute minimum.

The performance of the QI SC 1/3 & 2/3 included in Table 4 is illustrated in Table 5, where the errors when approximating the test functions are shown.

4.3. C^2 cubic quasi-interpolation

It is natural to ask whether the use of point values at knots and midpoints makes it possible to get C^2 cubic QIs exact on \mathbb{P}_3 . The following result holds.

Proposition 6. *There is no QIO exact on \mathbb{P}_3 that provides C^2 cubic QIs whose BB-coefficients*

	κ	λ	$\mu_\alpha, \alpha \in \{(3,0), (2,1), (1,2)\}$	UB
I	0	free	Depending on λ	
SC 1/2	$\frac{1}{384}$	free	Depending on λ	
I & SC 1/3	0	$-\frac{1}{27}$	$(0, 0, 1, 0, 0)$ $(\frac{1}{27}, -\frac{7}{27}, \frac{19}{18}, \frac{5}{27}, -\frac{1}{54})$ $(-\frac{1}{27}, \frac{7}{27}, \frac{17}{18}, -\frac{5}{27}, \frac{1}{54})$	$\frac{14}{9} = 1.556$
I & SC 2/3	0	$-\frac{1}{54}$	$(0, 0, 1, 0, 0)$ $(\frac{1}{54}, -\frac{5}{27}, \frac{17}{18}, \frac{7}{27}, -\frac{1}{27})$ $(-\frac{1}{54}, \frac{5}{27}, \frac{19}{18}, -\frac{7}{27}, \frac{1}{27})$	$\frac{14}{9} = 1.556$
SC 1/3 & 2/3	$\frac{1}{486}$	$-\frac{25}{972}$	$(\frac{1}{486}, -\frac{2}{243}, \frac{82}{81}, -\frac{2}{243}, \frac{1}{486})$ $(\frac{29}{972}, -\frac{56}{243}, \frac{82}{81}, \frac{52}{243}, -\frac{25}{972})$ $(-\frac{25}{972}, \frac{52}{243}, \frac{82}{81}, -\frac{56}{243}, \frac{29}{972})$	$\frac{245}{162} = 1.512$
NB	$-\frac{1}{18}$	$-\frac{1}{12}$	$(-\frac{1}{18}, \frac{1}{9}, \frac{1}{2}, \frac{5}{9}, -\frac{1}{9})$ $(-\frac{1}{12}, \frac{4}{9}, \frac{2}{3}, 0, -\frac{1}{36})$ $(-\frac{1}{36}, 0, \frac{2}{3}, \frac{4}{9}, -\frac{1}{12})$	$\frac{11}{9} = 1.222$

Table 4: Parameter values obtained by imposing on cubic QIs constructed from point values at knots the characteristics specified. The value of the upper bound (UB) of the infinity norm of the operator when its masks do not depend on any parameters is the reported in the last column. When masks do not depend on any parameter, they are given in the natural order $\mu_{(3,0)}$, $\mu_{(2,1)}$ and $\mu_{(2,2)}$.

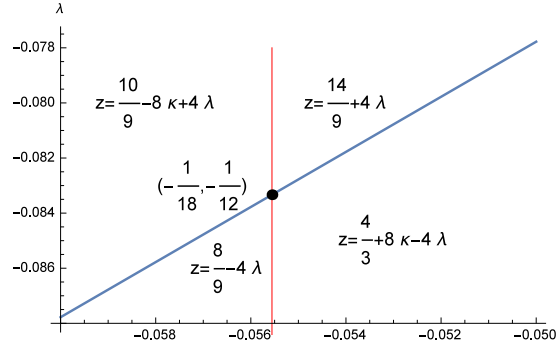


Figure 11: Representation of projection of the objective function in a neighbourhood of the point at which it reaches its absolute minimum.

n	f_1		f_2		f_3	
	error	NCO	error	NCO	error	NCO
16	3.46×10^{-2}		$2 - 92 \times 10^{-2}$		4.37×10^{-5}	
32	1.20×10^{-4}	4.846	1.94×10^{-3}	3.914	2.31×10^{-6}	4.241
64	3.14×10^{-5}	5.261	5.50×10^{-5}	5.137	1.45×10^{-7}	3.998
128	1.77×10^{-6}	4.149	2.37×10^{-6}	4.537	8.72×10^{-9}	4.053
256	1.11×10^{-7}	3.997	1.51×10^{-7}	3.974	5.78×10^{-10}	3.914

Table 5: Errors and NCOs for f_1 , f_2 and f_3 when the QI SC 1/3 & 2/3 is used.

have the structure given in (7). At most it is possible to reproduce \mathbb{P}_1 , in which case the masks are

$$\mu_{(3,0)} = \left(\frac{1}{6}, 0, \frac{2}{3}, 0, \frac{1}{6}\right), \quad \mu_{(2,1)} = \left(0, 0, \frac{2}{3}, 0, \frac{1}{3}\right), \quad \mu_{(1,2)} = \left(\frac{1}{3}, 0, \frac{2}{3}, 0, 0\right).$$

Proof. C^1 continuity at x_i is equivalent to the following conditions on the masks:

$$-2\mu_{(3,0),k} + \mu_{(2,1),k} + \mu_{(1,2),k} = 0, \quad k = 0, 1, 2, 4.$$

Moreover, C^2 continuity at x_i is obtained if and only if $\mu_{(2,1),0} = \mu_{(2,1),1} = \mu_{(1,2),3} = \mu_{(1,2),4} = 0$ and

$$\begin{aligned} 2\mu_{(1,2),0} - 2\mu_{(2,1),0} - \mu_{(2,1),2} &= 0, & 2\mu_{(1,2),1} - 2\mu_{(2,1),1} - \mu_{(2,1),3} &= 0, \\ \mu_{(1,2),0} + 2\mu_{(1,2),2} - 2\mu_{(2,1),2} - \mu_{(2,1),4} &= 0, & \mu_{(1,2),1} + 2\mu_{(1,2),3} - 2\mu_{(2,1),3} &= 0, \\ \mu_{(1,2),2} + 2\mu_{(1,2),4} - 2\mu_{(2,1),4} &= 0. \end{aligned}$$

The reproduction of the constants is equivalent to the conditions $\|\mu_\alpha\|_1 = 1$, $\alpha \in \{(3,0), (2,1), (1,2)\}$.

This system of equations has the unique solution given by

$$\mu_{(3,0)} = \left(\frac{1}{6}, 0, \frac{2}{3}, 0, \frac{1}{6}\right), \quad \mu_{(2,1)} = \left(0, 0, \frac{2}{3}, 0, \frac{1}{3}\right), \quad \mu_{(1,2)} = \left(\frac{1}{3}, 0, \frac{2}{3}, 0, 0\right).$$

It is straightforward to verify that these masks allow to reproduce also \mathbb{P}_1 but not \mathbb{P}_2 . \square

Note that, in fact, the QI associated with these masks only uses point values at the knots. Therefore, to improve the exactness we consider now point values at five knots:

$$b_{\alpha,i}(f) = \sum_{j=0}^4 \mu_{\alpha,j} f(x_{i+j-2}), \quad \alpha \in \{(3,0), (2,1), (1,2)\}. \quad (9)$$

Proposition 7. *The unique QIO $\mathcal{Q}_{3,2}^{\text{kn}}$ whose masks have the structure in (9) is given by the masks*

$$\mu_{(3,0)} = \left(-\frac{1}{36}, \frac{1}{9}, \frac{5}{6}, \frac{1}{9}, -\frac{1}{36}\right), \quad \mu_{(2,1)} = \left(0, -\frac{1}{9}, \frac{5}{6}, \frac{1}{3}, -\frac{1}{18}\right), \quad \mu_{(1,2)} = \left(0, -\frac{1}{18}, \frac{1}{3}, \frac{5}{6}, -\frac{1}{9}\right).$$

Proof. The C^2 continuity at x_i of $\mathcal{Q}_{3,2}^{\text{kn}}f$ is equivalent to the fulfillment of the following equations: $\mu_{(1,2),4} = \mu_{(2,1),0} = 0$, $\mu_{(1,2),k} - 2\mu_{(3,0),k} + \mu_{(2,1),k} = 0$ for $k = 0, 1, 2, 3, 4$, and

$$\begin{aligned} 2\mu_{(1,2),0} - 2\mu_{(2,1),0} - \mu_{(2,1),1} &= 0, & \mu_{(1,2),0} + 2\mu_{(1,2),1} - 2\mu_{(2,1),1} - \mu_{(2,1),2} &= 0, \\ \mu_{(1,2),1} + 2\mu_{(1,2),2} - 2\mu_{(2,1),2} - \mu_{(2,1),3} &= 0, & \mu_{(1,2),3} + 2\mu_{(1,2),4} - 2\mu_{(2,1),4} &= 0, \\ \mu_{(1,2),2} + 2\mu_{(1,2),3} - 2\mu_{(2,1),3} - \mu_{(2,1),4} &= 0. \end{aligned}$$

This system of equations has the unique solution given in the statement. \square

The BB-coefficients in the interval I_i of $\mathcal{Q}_{3,2}^{\text{kn}}f$ are

$$\begin{aligned} b_{(3,0),i}(f) &= \frac{1}{36} (-f(x_{i-2}) + 4f(x_{i-1}) + 30f(x_i) + 4f(x_{i+1}) - f(x_{i+2})), \\ b_{(2,1),i}(f) &= \frac{1}{18} (-2f(x_{i-1}) + 15f(x_i) + 6f(x_{i+1}) - f(x_{i+2})), \\ b_{(1,2),i}(f) &= \frac{1}{18} (-f(x_{i-1}) + 6f(x_i) + 15f(x_{i+1}) - 2f(x_{i+2})), \\ b_{(0,3),i}(f) &= \frac{1}{36} (-f(x_{i-1}) + 4f(x_i) + 30f(x_{i+1}) + 4f(x_{i+2}) - f(x_{i+3})). \end{aligned}$$

Remark 4. *By dealing with the BB-coefficients of the C^2 cubic B-spline M_4 centered at the origin, it is easy to prove that the QI we have obtained coincides with the classical QI (see [16])*

$$Qf = \sum_{i \in \mathbb{Z}} \frac{1}{6} (-f(a+h(i-1)) + 8f(a+hi) - f(a+h(i+1))) M_4\left(\frac{\cdot - a}{h} - i\right).$$

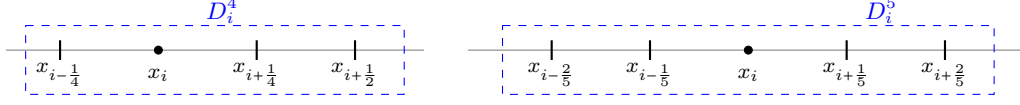


Figure 12: The sets D_i^4 and D_i^5 providing suitable partitions of the set formed by the domain points in the quartic and quintic cases.

5. C^1 and C^2 quartic and quintic quasi-interpolation

We complete the results on low-degree QI by providing the BB-coefficients of the QIs corresponding to the masks associated with specific subsets D_i , as more symmetrical with respect to x_i as possible. As there are five (resp. six) domain points in I_i in the quartic (resp. quintic) case, we choose the subsets D_i^4 and D_i^5 shown in Figure 12 to define C^1 and C^2 quartic and quintic QIs by setting their BB-coefficients relative to the interval I_i .

5.1. The C^1 quartic case

If the point values are known at the knots and midpoints, then again the BB-coefficients associated with the points in D_i^4 will be calculated from $f(x_{i+\frac{j}{2}})$, $j = -2, -1, 0, 1, 2$.

Proposition 8. *Under the above conditions, the only operator $\mathcal{Q}_{4,1}$ which is exact on \mathbb{P}_4 and produces C^1 QIs is defined from the masks $\mu_{(4,0)} = (0, 0, 1, 0, 0)$, $\mu_{(3,1)} = (\frac{1}{24}, -\frac{1}{3}, 1, \frac{1}{3}, -\frac{1}{24})$, $\mu_{(2,2)} = (\frac{1}{18}, -\frac{2}{9}, \frac{1}{6}, \frac{10}{9}, -\frac{1}{9})$ and $\mu_{(1,3)} = (-\frac{1}{24}, \frac{1}{3}, 1, -\frac{1}{3}, \frac{1}{24})$.*

Proof. C^1 continuity at x_i is achieved if and only if

$$b_{(4,0),i}(f) = \frac{1}{2} (b_{(1,3),i-1}(f) + b_{(3,1),i}(f)),$$

which is equivalent to the equations $\mu_{(1,3),k} - 2\mu_{(4,0),k} + \mu_{(3,1),k} = 0$, $0 \leq k \leq 4$. Imposing that the BB-coefficients of the monomials $m_\ell(x) = x^\ell$, $0 \leq \ell \leq 4$, as polynomials of degree four, are equal to those of $\mathcal{Q}_{4,1}m_\ell$, the exactness of $\mathcal{Q}_{4,1}$ on \mathbb{P}_4 is obtained if and only if the equalities $\|\mu_\alpha\|_1 = 1$, $\alpha \in \{(4,0), (3,1), (2,2), (1,2)\}$ hold, as well as

$$\begin{aligned} 16\mu_{(4,0),0} + \mu_{(4,0),1} + \mu_{(4,0),3} + 16\mu_{(4,0),4} &= 0, & -8\mu_{(4,0),0} - \mu_{(4,0),1} + \mu_{(4,0),3} + 8\mu_{(4,0),4} &= 0, \\ 4\mu_{(4,0),0} + \mu_{(4,0),1} + \mu_{(4,0),3} + 4\mu_{(4,0),4} &= 0, & -2\mu_{(4,0),0} - \mu_{(4,0),1} + \mu_{(4,0),3} + 2\mu_{(4,0),4} &= 0, \\ \mu_{(4,0),1} + 2\mu_{(4,0),2} + 3\mu_{(4,0),3} + 4\mu_{(4,0),4} &= 2, & \mu_{(4,0),1} + 4\mu_{(4,0),2} + 9\mu_{(4,0),3} + 16\mu_{(4,0),4} &= 4, \\ \mu_{(4,0),1} + 8\mu_{(4,0),2} + 27\mu_{(4,0),3} + 64\mu_{(4,0),4} &= 8, & \mu_{(4,0),1} + 16\mu_{(4,0),2} + 81\mu_{(4,0),3} + 256\mu_{(4,0),4} &= 16, \\ 16\mu_{(3,1),0} + \mu_{(3,1),1} + \mu_{(3,1),3} + 16\mu_{(3,1),4} &= 0, & -8\mu_{(3,1),0} - \mu_{(3,1),1} + \mu_{(3,1),3} + 8\mu_{(3,1),4} &= 0, \\ 4\mu_{(3,1),0} + \mu_{(3,1),1} + \mu_{(3,1),3} + 4\mu_{(3,1),4} &= 0, & -2\mu_{(3,1),0} - \mu_{(3,1),1} + \mu_{(3,1),3} + 2\mu_{(3,1),4} &= 1/2, \\ 16\mu_{(2,2),0} + \mu_{(2,2),1} + \mu_{(2,2),3} + 16\mu_{(2,2),4} &= 0, & -8\mu_{(2,2),0} - \mu_{(2,2),1} + \mu_{(2,2),3} + 8\mu_{(2,2),4} &= 0, \\ 4\mu_{(2,2),0} + \mu_{(2,2),1} + \mu_{(2,2),3} + 4\mu_{(2,2),4} &= 2/3, & -2\mu_{(2,2),0} - \mu_{(2,2),1} + \mu_{(2,2),3} + 2\mu_{(2,2),4} &= 1, \\ \mu_{(1,3),1} + 2\mu_{(1,3),2} + 3\mu_{(1,3),3} + 4\mu_{(1,3),4} &= 3/2, & \mu_{(1,3),1} + 4\mu_{(1,3),2} + 9\mu_{(1,3),3} + 16\mu_{(1,3),4} &= 2, \\ \mu_{(1,3),1} + 8\mu_{(1,3),2} + 27\mu_{(1,3),3} + 64\mu_{(1,3),4} &= 2, & \mu_{(1,3),1} + 16\mu_{(1,3),2} + 81\mu_{(1,3),3} + 256\mu_{(1,3),4} &= 0. \end{aligned}$$

This system of 29 equations has only one solution, which gives the masks of the statement. \square

Remark 5. *Note that $\mathcal{Q}_{4,1}f$ interpolates f at the knots.*

If it is assumed that only the point values at the knots are known, then $f(x_{i+j})$, $j = -2, -1, 0, 1, 2$, will be used to calculate the masks with which the BB-coefficients are formed. We have the following result, which is proved in a completely analogous way.

Proposition 9. *Under the above conditions, the only operator $\mathcal{Q}_{4,1}^{kn}$ which is exact on \mathbb{P}_4 and which produces C^1 QIs is defined from the masks $\mu_{(4,0)} = (0, 0, 1, 0, 0)$, $\mu_{(3,1)} = (\frac{1}{48}, -\frac{1}{6}, 1, \frac{1}{6}, -\frac{1}{48})$, $\mu_{(2,2)} = (\frac{5}{144}, -\frac{2}{9}, \frac{19}{24}, \frac{4}{9}, -\frac{7}{144})$ and $\mu_{(1,3)} = (-\frac{1}{48}, \frac{1}{6}, 1, -\frac{1}{6}, \frac{1}{48})$.*

n	f_1		f_2		f_3	
	error	NCO	error	NCO	error	NCO
16	4.74×10^{-3}		5.94×10^{-3}		7.03×10^{-6}	
32	1.67×10^{-4}	4.826	3.07×10^{-4}	4.276	2.24×10^{-7}	4.972
64	4.90×10^{-6}	5.093	9.20×10^{-6}	5.060	6.98×10^{-9}	5.005
128	1.52×10^{-7}	5.012	2.72×10^{-7}	5.079	2.18×10^{-10}	5.000
256	4.83×10^{-9}	4.977	8.81×10^{-9}	4.949	7.10×10^{-12}	4.940
n	error	NCO	error	NCO	error	NCO
16	3.59×10^{-2}		3.66×10^{-2}		7.70×10^{-5}	
32	1.69×10^{-3}	4.406	3.01×10^{-3}	3.603	2.56×10^{-6}	4.911
64	5.68×10^{-5}	4.897	9.67×10^{-5}	4.960	8.16×10^{-8}	4.971
128	1.77×10^{-6}	5.007	3.04×10^{-6}	4.992	2.44×10^{-9}	5.063
256	5.46×10^{-8}	5.017	1.01×10^{-7}	4.910	7.87×10^{-11}	4.954

Table 6: Errors and NCOs for f_1 , f_2 and f_3 when the QIs in Propositions 8 and 9 are used.

This result shows that, in fact, also $\mathcal{Q}_{4,1}^{\text{kn}} f$ interpolates f at the knots.

Table 6 illustrates the performance of the QIs given in Propositions 8 and 9. The first part corresponds to BB-coefficients defined from point values at five knots and midpoints. In the second one seven point values at knots are used. The results are in good agreement with the theoretical ones.

5.2. The C^2 quartic case

As far as class C^2 is concerned, when the values at knots and midpoints are assumed to be known, it is not possible to reproduce \mathbb{P}_4 but \mathbb{P}_3 using masks in \mathbb{R}^5 . They are

$$\begin{aligned} \mu_{(4,0)} &= (\kappa, -4\kappa, 1 + 6\kappa, -4\kappa, \kappa), & \mu_{(3,1)} &= \left(\frac{1}{24} + \kappa, -\frac{1}{3} - 4\kappa, 1 + 6\kappa, \frac{1}{3} - 4\kappa, -\frac{1}{24} + \kappa \right), \\ \mu_{(2,2)} &= \left(0, 0, -\frac{1}{6}, \frac{4}{3}, -\frac{1}{6} \right), & \mu_{(1,3)} &= \left(-\frac{1}{24} + \kappa, \frac{1}{3} - 4\kappa, 1 + 6\kappa, -\frac{1}{3} - 4\kappa, \frac{1}{24} + \kappa \right). \end{aligned}$$

They yield a family of operators $\mathcal{Q}_{4,2,3}$. The value $\kappa = 0$ produces quasi-interpolating splines interpolatory at the knots. Any value $\kappa \in [-\frac{1}{6}, -\frac{1}{72}]$ gives rise to masks providing an operator such that the upper bound of its infinity norm (defined as above) is minimal (and equal to $5/3$).

To achieve exactness on \mathbb{P}_4 it is necessary to define the BB-coefficients from at least seven evaluations at knots and midpoints, which we will choose as close as possible to x_i and symmetrically distributed around it. In this case we obtain the following family of masks satisfying the required conditions:

$$\begin{aligned} \mu_{(4,0)} &= \left(\kappa, -3\kappa - \frac{\lambda}{5}, \lambda, 1 + 10\kappa - 2\lambda, -15\kappa + 2\kappa, -9\kappa - \lambda, -2\kappa + \frac{\lambda}{5} \right), \\ \mu_{(3,1)} &= \left(-\frac{1}{72} + \kappa, \frac{7}{72} - 3\kappa - \frac{\lambda}{5}, -\frac{29}{72} + \lambda, 1 + 10\kappa - 2\lambda, \frac{29}{72} - 15\kappa + 2\lambda, -\frac{7}{72} + 9\kappa - \lambda, \frac{1}{72} - 2\kappa + \frac{\lambda}{5} \right), \\ \mu_{(2,2)} &= \left(0, 0, \frac{1}{18}, -\frac{7}{18}, \frac{5}{3}, -\frac{7}{18}, \frac{1}{18} \right), \\ \mu_{(1,3)} &= \left(\frac{1}{72} + \kappa, -\frac{7}{72} - 3\kappa - \frac{\lambda}{5}, \frac{29}{72} + \lambda, 1 + 10\kappa - 2\lambda, -\frac{29}{72} - 15\kappa + 2\lambda, \frac{7}{72} + 9\kappa - \lambda, -\frac{1}{72} - 2\kappa + \frac{\lambda}{5} \right). \end{aligned}$$

If the parameters are zero, then the QI interpolates at the knots and, moreover, is superconvergent at the midpoints, i.e.,

$$\left| \frac{1}{16} (b_{(4,0),i}(f) + 4b_{(3,1),i}(f) + 6b_{(2,2),i}(f) + 4b_{(1,3),i}(f) + b_{(0,4),i}(f)) - f(x_{i+\frac{1}{2}}) \right| = \mathcal{O}(h^6).$$

In this case, the masks are

$$\begin{aligned} \mu_{(4,0)} &= (0, 0, 0, 1, 0, 0, 0), & \mu_{(3,1)} &= \left(-\frac{1}{72}, \frac{7}{72}, -\frac{29}{72}, 1, \frac{29}{72}, -\frac{7}{72}, \frac{1}{72} \right), \\ \mu_{(2,2)} &= \left(0, 0, \frac{1}{18}, -\frac{7}{18}, \frac{5}{3}, -\frac{7}{18}, \frac{1}{18} \right), & \mu_{(1,3)} &= \left(\frac{1}{72}, -\frac{7}{72}, \frac{29}{72}, 1, -\frac{29}{72}, \frac{7}{72}, -\frac{1}{72} \right). \end{aligned}$$

n	f_1		f_2		f_3	
	error	NCO	error	NCO	error	NCO
16	4.75×10^{-3}		5.94×10^{-3}		7.03×10^{-6}	
32	1.67×10^{-4}	4.826	3.07×10^{-4}	4.276	2.24×10^{-7}	4.972
64	4.90×10^{-6}	5.093	9.20×10^{-6}	5.060	6.98×10^{-9}	5.005
128	1.52×10^{-7}	5.012	2.72×10^{-7}	5.080	2.18×10^{-10}	5.000
256	4.83×10^{-9}	4.977	8.81×10^{-9}	4.950	7.10×10^{-12}	4.940

Table 7: Errors and NCOs provided by the superconvergent at midpoints and interpolatory at knots C^2 quartic QI exact on \mathbb{P}_4 when it is applied to f_1 , f_2 and f_3 .

Table 7 shows the errors and NCOs when the previous C^2 quartic QI is applied to the test functions. Also in this case, the results are satisfactory.

When it is assumed that only the values at the nodes are known, and the BB-coefficients are defined from the values $f(x_{i+j})$, $j = -2, -1, 0, 1, 2$, exactness can only be achieved on \mathbb{P}_3 , and the following uniparametric family of masks is found:

$$\begin{aligned} \mu_{(4,0)} &= (\kappa, -4\kappa, 1 + 6\kappa, -4\kappa, \kappa), \quad \mu_{(3,1)} = \left(\frac{1}{48} + \kappa, -\frac{1}{6} - 4\kappa, 1 + 6\kappa, \frac{1}{6} - 4\kappa, -\frac{1}{48} + \kappa \right), \\ \mu_{(2,2)} &= \left(0, -\frac{1}{12}, \frac{7}{12}, \frac{7}{12}, -\frac{1}{12} \right), \quad \mu_{(1,3)} = \left(-\frac{1}{48} + \kappa, \frac{1}{6} - 4\kappa, 1 + 6\kappa, -\frac{1}{6} - 4\kappa, \frac{1}{48} + \kappa \right). \end{aligned}$$

Again, the value $\kappa = 0$ gives rise to approximants that interpolate at the nodes. Any value $\kappa \in \left[-\frac{1}{12}, -\frac{1}{144}\right]$ leads to masks that provide an operator such that the upper bound of its infinity norm is minimal, found to be equal to $4/3$, so it has been reduced relative to that obtained using values at nodes and midpoints.

Finally, to construct C^2 quartic QIs exact on \mathbb{P}_4 , we define the BB-coefficients from masks in \mathbb{R}^7 . In this case, a 3-parametric family of masks is obtained, namely

$$\begin{aligned} \mu_{(4,0)} &= (\kappa, \lambda, -5(3\kappa + \lambda), 1 + 40\kappa + 10\lambda, -5(9\kappa + 2\lambda), 24\kappa + 5\lambda, -5\kappa - \lambda), \\ \mu_{(3,1)} &= \left(-\theta + 2\kappa, \frac{7}{576} + 6\theta - 6\kappa + \lambda, -\frac{71}{576} - 15\theta - 5\lambda, \frac{263}{288} + 20\theta + 20\kappa + 10\lambda, \right. \\ &\quad \left. \frac{73}{288} - 15\theta - 30\kappa - 10\lambda, -\frac{37}{576} + 6\theta + 18\kappa + 5\lambda, \frac{5}{576} - \theta - 4\kappa - \lambda \right), \\ \mu_{(2,2)} &= \left(0, 4(\theta - \kappa) \cdot -\frac{7}{144} - 20\theta + 20\kappa, \frac{4}{9} + 40\theta - 40\kappa, \frac{19}{24} - 40\theta + 40\kappa, -\frac{2}{9} + 20\theta - 20\kappa, \frac{5}{144} - 4\theta + 4\kappa \right), \\ \mu_{(1,3)} &= \left(-\theta + 2\kappa, \frac{7}{576} + 6\theta - 6\kappa, -\frac{71}{576} - 15\theta - 15\lambda, \frac{263}{288} + 20\theta + 20\kappa + 10\lambda, \frac{73}{288} - 15\theta - 30\kappa - 10\lambda, \right. \\ &\quad \left. -\frac{37}{576} + 6\theta + 18\kappa + 5\lambda, \frac{5}{576} - \theta - 4\kappa - \lambda \right). \end{aligned}$$

Taking into account the structure of the resulting masks in the cases analysed so far, we determine specific parameter values by imposing the following conditions:

1. $\mu_{(4,0)}$ is symmetric, i.e. $\mu_{(4,0),k} = \mu_{(4,0),7-k}$, $0 \leq k \leq 3$. It will be satisfied if $\lambda = -6\kappa$.
2. Applying the above condition, it will be required that $\mu_{(2,2),2}$ and $\mu_{(2,2),7}$ be equal. It will be fulfilled if $\kappa = \theta - \frac{5}{1152}$.
3. Under the above conditions, it will be requested that $\mu_{(1,3),1} = -\mu_{(1,3),7}$. It will be achieved if $\theta = \frac{5}{1152}$.

Successive application of these conditions produces the values $\theta_0 = \frac{5}{1152}$, $\kappa_0 = 0$ and $\lambda_0 = -\frac{5}{192}$, and the following masks:

$$\begin{aligned} \mu_{(4,0)}^{\theta_0, \kappa_0, \lambda_0} &= (0, 0, 0, 1, 0, 0, 0), \\ \mu_{(3,1)}^{\theta_0, \kappa_0, \lambda_0} &= \mu_{(1,3)}^{\theta_0, \kappa_0, \lambda_0} = \left(-\frac{5}{1152}, \frac{11}{288}, -\frac{217}{1152}, 1, \frac{217}{1152}, -\frac{11}{288}, \frac{5}{1152} \right), \\ \mu_{(2,2)}^{\theta_0, \kappa_0, \lambda_0} &= \left(0, \frac{5}{288}, -\frac{13}{96}, \frac{89}{144}, \frac{89}{144}, -\frac{13}{96}, \frac{5}{288} \right). \end{aligned}$$

n	f_1		f_2		f_3	
	error	NCO	error	NCO	error	NCO
16	3.59×10^{-2}		3.66×10^{-2}		7.70×10^{-5}	
32	1.69×10^{-3}	4.406	3.01×10^{-3}	3.603	2.56×10^{-6}	4.912
64	5.68×10^{-5}	4.897	9.66×10^{-5}	4.960	8.16×10^{-8}	4.971
128	1.77×10^{-6}	5.007	3.04×10^{-6}	4.992	2.44×10^{-9}	5.063
256	5.46×10^{-8}	5.017	1.01×10^{-7}	4.910	7.87×10^{-11}	4.954

Table 8: Errors and NCOs obtained when the QIO associated with the masks $\mu_\alpha^{\theta_0, \kappa_0, \lambda_0}$, $|a| = 4$, is applied to the test functions.

Once again, the quasi-interpolating spline interpolates at the knots. The results in Table 8 illustrate the performance of the operator defined from masks $\mu_\alpha^{\theta_0, \kappa_0, \lambda_0}$, $|a| = 4$.

5.3. The quintic case

The construction of quintic QIs exact on \mathbb{P}_5 is carried out in the same way. As indicated above, it is sufficient to define the BB-coefficients associated with the domain points in D_i^5 . As far as the C^1 regularity is concerned, point evaluations at seven knots and midpoints symmetrically distributed around x_i are considered. The following result is obtained.

Proposition 10. *The following 4-parametric family of masks provides operators exact on \mathbb{P}_5 producing C^1 quintic QIs:*

$$\begin{aligned}
\mu_{(5,0)} &= (\kappa, -6\kappa, 15\kappa, 1 - 20\kappa, 15\kappa, -6\kappa, \kappa), \\
\mu_{(4,1)} &= \left(2\kappa - \lambda, -12\kappa + 6\lambda + \frac{1}{50}, 30\kappa - 15\lambda - \frac{1}{5}, -40\kappa + 20\lambda + \frac{13}{15}, \right. \\
&\quad \left. 30\kappa - 15\lambda + \frac{2}{5}, -12\kappa + 6\lambda - \frac{1}{10}, 2\kappa - \lambda + \frac{1}{75} \right), \\
\mu_{(3,2)} &= \left(\nu, -6\nu + \frac{7}{300}, 15\nu - \frac{2}{15}, -20\nu + \frac{7}{30}, 15\nu + \frac{16}{15}, -6\nu - \frac{13}{60}, \nu + \frac{2}{75} \right), \\
\mu_{(2,3)} &= \left(\xi, -6\xi - \frac{17}{300}, 15\xi + \frac{2}{3}, -20\xi + \frac{23}{20}, 15\xi - \frac{8}{15}, -6\xi + \frac{11}{60}, \xi - \frac{2}{75} \right), \\
\mu_{(1,4)} &= \left(\lambda, -6\lambda - \frac{1}{50}, 15\lambda + \frac{1}{5}, -20\lambda + \frac{17}{15}, 15\lambda - \frac{2}{5}, -6\lambda + \frac{1}{10}, \lambda - \frac{1}{75} \right),
\end{aligned}$$

$$\kappa, \lambda, \nu, \xi \in \mathbb{R}.$$

Again, we have parameters that can be chosen so that the QIs satisfy specific properties. The following conditions are imposed consecutively.

1. Interpolation at knots, i.e., $\kappa = 0$.
2. $\mu_{(3,2),k} = \mu_{(2,3),6-k}$, $0 \leq k \leq 6$. It will be fulfilled if $\nu = \xi - \frac{2}{75}$.
3. Under the above conditions, it will be required that $\mu_{(1,4),k} = \mu_{(4,1),6-k}$, $0 \leq k \leq 3$. It will be satisfied if $\lambda = \frac{1}{150}$.

This procedure leads to constant masks $\mu_{(5,0)}^\xi = (0, 0, 0, 1, 0, 0, 0)$,

$$\mu_{(4,1)}^\xi = \left(-\frac{1}{150}, \frac{3}{50}, -\frac{3}{10}, 1, \frac{3}{10}, -\frac{3}{50}, \frac{1}{150} \right) \quad \text{and} \quad \mu_{(1,4)}^\xi = \left(\frac{1}{150}, -\frac{3}{50}, \frac{3}{10}, 1, -\frac{3}{10}, \frac{3}{50}, -\frac{1}{50} \right),$$

and two remaining ones depending on ξ , namely,

$$\mu_{(3,2)}^\xi = \left(-\frac{2}{57} + \xi, \frac{11}{60} - 6\xi, -\frac{8}{15} + 15\xi, \frac{23}{30} - 20\xi, \frac{2}{3} + 15\xi, -\frac{17}{300} - 6\xi, \xi \right)$$

and

$$\mu_{(2,3)}^\xi = \left(\xi, -\frac{17}{300} - 6\xi, \frac{2}{3} + 15\xi, \frac{23}{30} - 20\xi, -\frac{8}{15} + 15\xi, \frac{11}{60} - 6\xi, \xi - \frac{2}{75} \right).$$

n	f_1		f_2		f_3	
	error	NCO	error	NCO	error	NCO
16	1.67×10^{-2}		9.76×10^{-4}		7.98×10^{-8}	
32	1.13×10^{-5}	7.210	2.10×10^{-5}	5.539	6.77×10^{-10}	6.881
64	6.97×10^{-8}	7.340	1.03×10^{-7}	7.312	7.18×10^{-12}	6.558
128	5.83×10^{-10}	6.901	1.03×10^{-9}	7.007	9.33×10^{-14}	6.267
256	5.72×10^{-12}	6.671	1.42×10^{-11}	6.490	1.34×10^{-15}	6.120

Table 9: Errors and NCOs obtained when the QIO associated with the masks $\mu_\alpha^{\frac{1}{75}}$, $|\alpha| = 5$, is applied to the test functions.

The parameter ξ can be chosen by requiring an additional condition. A first option is to impose that the upper bound

$$\max \left\{ \frac{26}{15}, \left| \frac{23}{30} - 20\xi \right| + \left| \frac{17}{300} + 6\xi \right| + \left| \frac{11}{60} - 6\xi \right| + \left| \frac{2}{75} - \xi \right| + |\xi| + \left| \frac{8}{15} - 15\xi \right| + \left| \frac{2}{3} + 15\xi \right| \right\}$$

of the infinity norm of the operator $\mathcal{Q}_{5,1,5}^\xi$ provided by those masks be minimal. Calculations similar to those carried out in the quadratic case allow to conclude that the minimum of this objective function, which is equal to $\frac{26}{15}$, is reached for all values of the parameter ξ in the small interval $[\frac{1}{40}, \frac{63}{1600}]$. There is no privileged choice of the parameter in this interval.

A second option is to require that the QIO \mathcal{Q}^ξ be superconvergent at the midpoints, i.e. such

$$\left| \mathcal{Q}_{5,1,5}^\xi f \left(x_{i+\frac{1}{2}} \right) - f \left(x_{i+\frac{1}{2}} \right) \right| = \left| \frac{1}{32} \sum_{\ell=0}^5 \binom{5}{\ell} b_{(5-\ell, \ell)}^\xi (f) - f \left(x_{i+\frac{1}{2}} \right) \right| = \mathcal{O}(h^r)$$

with $r > 6$. After some computations it is obtained this result with $r = 7$ for $\xi = \frac{1}{75}$. The corresponding masks of the resulting operator $\mathcal{Q}_{5,1,5}^{\frac{1}{75}}$ are

$$\begin{aligned} \mu_{(5,0)}^{\frac{1}{75}} &= (0, 0, 0, 1, 0, 0, 0), & \mu_{(4,1)}^{\frac{1}{75}} &= \left(-\frac{1}{150}, \frac{3}{50}, -\frac{3}{10}, 1, \frac{3}{10}, -\frac{3}{50}, \frac{1}{150} \right), \\ \mu_{(3,2)}^{\frac{1}{75}} &= \left(-\frac{1}{75}, \frac{31}{300}, -\frac{1}{3}, \frac{1}{2}, \frac{13}{15}, -\frac{41}{300}, \frac{1}{75} \right), & \mu_{(2,3)}^{\frac{1}{75}} &= \left(\frac{1}{75}, -\frac{41}{300}, \frac{13}{15}, \frac{1}{2}, -\frac{1}{3}, -\frac{31}{300}, -\frac{1}{75} \right) \end{aligned}$$

and $\mu_{(1,4)}^{\frac{1}{75}} = \left(\frac{1}{150}, -\frac{3}{50}, \frac{3}{10}, 1, -\frac{3}{10}, \frac{3}{50}, -\frac{1}{150} \right)$. The errors and NCOs resulting when $\mathcal{Q}_{5,1,5}^{\frac{1}{75}}$ is applied to the three test functions are shown in Table 9.

Working as before, the following result can be proved.

Proposition 11. *If only point values at five symmetrically distributed knots and midpoints around a knot are used, then exactness can only be achieved on \mathbb{P}_4 , existing only a unique set of masks that produce C^1 regularity:*

$$\begin{aligned} \mu_{(5,0)} &= (0, 0, 1, 0, 0), & \mu_{(4,1)} &= \left(\frac{1}{30}, -\frac{4}{15}, 1, \frac{4}{15}, -\frac{1}{30} \right), & \mu_{(3,2)} &= \left(\frac{1}{20}, -\frac{4}{15}, 1, \frac{4}{15}, -\frac{1}{12} \right), \\ \mu_{(2,3)} &= \left(-\frac{1}{12}, \frac{4}{5}, \frac{1}{2}, -\frac{4}{15}, \frac{1}{20} \right), & \mu_{(1,4)} &= \left(-\frac{1}{30}, \frac{4}{15}, 1, -\frac{4}{15}, \frac{1}{30} \right). \end{aligned}$$

Note that the resulting quasi-interpolating spline is interpolatory at knots.

Remark 6. *The masks μ_α^ξ , $\xi \in \mathbb{R}$, give rise to C^2 quintic QIs.*

To study the C^2 quintic cases we will follow the same procedure. When the BB-coefficients are defined from values at knots and midpoints or only at knots, the general family of masks ensuring exactness on \mathbb{P}_5 and C^2 regularity depends on two parameters. They are

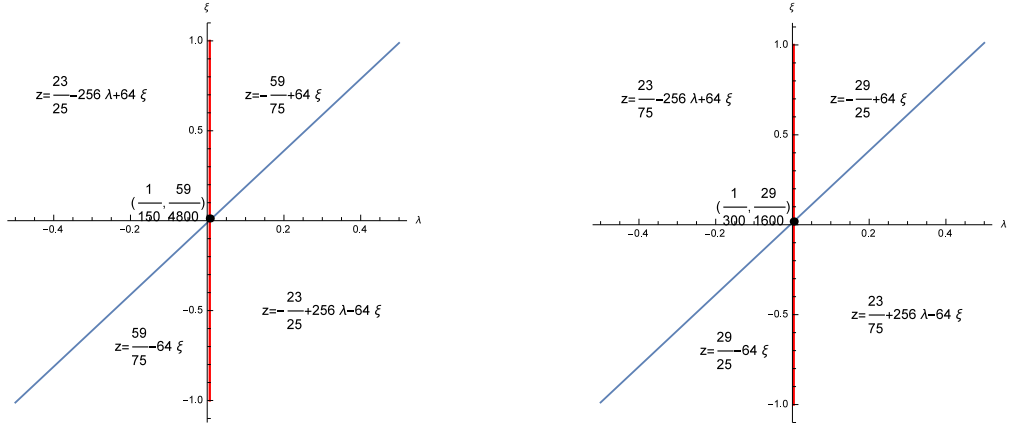


Figure 13: Projections of the graphs of the objective functions in neighbourhoods of the points where they reach their absolute minimum values. They are determined as intersection of four planes.

$$\begin{aligned}
\mu_{(5,0)} &= (\kappa, -6\kappa, 15\kappa, 1 - 20\kappa, 15\kappa, -6\kappa, \kappa), \\
\mu_{(4,1)} &= (-\kappa + 2\lambda, p_1 + 6\kappa - 12\lambda, p_2 - 15\kappa + 30\lambda, p_3 + 20\kappa - 40\lambda, p_4 - 15\kappa + 30\lambda, \\
&\quad p_5 + 6\kappa - 12\lambda, p_6 - \kappa + 2\lambda), \\
\mu_{(3,2)} &= (-4\kappa + 4\lambda + \xi, p_7 + 24\kappa - 24\lambda - 6\xi, p_8 - 60\kappa + 60\lambda + 15\xi, p_9 + 80\kappa - 80\lambda - 20\xi, \\
&\quad p_{10} - 60\kappa + 60\lambda + 15\xi, p_{11} + 24\kappa - 24\lambda - 6\xi, p_{12} - 4\kappa + 4\lambda + \xi), \\
\mu_{(2,3)} &= (\xi, p_{13} - 6\xi, p_{14} + 15\xi, p_{15} - 20\xi, p_{16} + 15\xi, p_{17} - 6\xi, p_{18} + \xi), \\
\mu_{(1,4)} &= (\kappa, p_{19} - 6\kappa, p_{20} + 15\kappa, p_{21} - 20\kappa, p_{22} + 15\kappa, p_{23} - 6\kappa, p_{24} + \kappa),
\end{aligned}$$

where the entries of the $p := (p_i)_{1 \leq i \leq 24}$ depend on the type of data used to define the BB-coefficients. When using point values at knots and midpoints, then

$$p = \left(\frac{1}{50}, -\frac{1}{5}, \frac{13}{15}, \frac{2}{5}, -\frac{1}{10}, \frac{1}{75}, \frac{7}{300}, -\frac{2}{15}, \frac{7}{30}, \frac{16}{15}, -\frac{13}{60}, \frac{2}{75}, -\frac{17}{300}, \frac{2}{3}, \frac{23}{30}, -\frac{8}{15}, \frac{11}{60}, -\frac{2}{75}, \frac{1}{50}, \frac{1}{5}, \frac{17}{15}, -\frac{2}{5}, \frac{1}{10}, -\frac{1}{75} \right)$$

and

$$p = \left(\frac{1}{100}, \frac{-1}{10}, \frac{14}{15}, \frac{1}{5}, \frac{-1}{20}, \frac{1}{150}, \frac{19}{1200}, \frac{-2}{15}, \frac{89}{120}, \frac{7}{15}, \frac{-5}{48}, \frac{1}{75}, \frac{-29}{1200}, \frac{4}{15}, \frac{121}{120}, \frac{-1}{3}, \frac{23}{240}, \frac{-1}{75}, \frac{-1}{100}, \frac{1}{10}, \frac{16}{15}, \frac{-1}{5}, \frac{1}{20}, \frac{-1}{150} \right)$$

if only point values at knots are involved.

As in some previous cases, the mask relative to the vertices depends only on the parameter κ , whether values are used at the knots and at the midpoints or only at the knots. If this parameter is set to zero, it leads to QIs that interpolate at the knots, in whose masks only the parameters λ and ξ are involved. The infinity norm of each of the corresponding operators is bounded by a convex function defined from the 1-norms of the masks, and depends only those parameters. They attain their minimum values at unique points. Figure 13 shows the very similar structures of both functions.

Using point values at knots and midpoints, the minimum value (equal to $\frac{159}{80}$) is reached at $\lambda_1 = \frac{1}{150}$ and $\xi_1 = \frac{59}{4800}$. The masks of the resulting operator $\mathcal{Q}_{5,2,5}^{0,\lambda_1,\xi_1}$ are

$$\begin{aligned}
\mu_{(5,0)}^{0,\lambda_1,\xi_1} &= (0, 0, 0, 1, 0, 0, 0), \\
\mu_{(4,1)}^{0,\lambda_1,\xi_1} &= \left(-\frac{1}{150}, \frac{3}{50}, -\frac{3}{10}, 1, \frac{3}{10}, -\frac{3}{50}, \frac{1}{150} \right), \quad \mu_{(1,3)}^{0,\lambda_1,\xi_1} = \left(\frac{1}{150}, -\frac{3}{50}, \frac{3}{10}, 1, -\frac{3}{10}, \frac{3}{50}, -\frac{1}{150} \right), \\
\mu_{(3,2)}^{0,\lambda_1,\xi_1} &= \left(-\frac{23}{1600}, \frac{263}{2400}, -\frac{67}{192}, \frac{25}{48}, \frac{817}{960}, -\frac{313}{2400}, \frac{59}{4800} \right), \quad \mu_{(2,3)}^{0,\lambda_1,\xi_1} = \left(\frac{59}{4800}, -\frac{313}{2400}, \frac{817}{960}, \frac{25}{48}, -\frac{67}{192}, \frac{263}{2400}, -\frac{23}{1600} \right).
\end{aligned}$$

When only point values at knots are used, the minimum value (equal to $\frac{679}{480}$) is attained at

$\lambda_2 = \frac{1}{300}$ and $\xi_2 = \frac{29}{1600}$. The masks of $\mathcal{Q}_{5,2,5}^{\text{kn},0,\lambda_2,\xi_2}$ are

$$\begin{aligned} \mu_{(5,0)}^{\text{kn},0,\lambda_2,\xi_2} &= (0, 0, 0, 1, 0, 0, 0), \\ \mu_{(4,1)}^{\text{kn}}, 0, \lambda_2, \xi_2 &= \left(-\frac{1}{300}, \frac{3}{100}, -\frac{3}{20}, 1, \frac{3}{20}, -\frac{3}{100}, \frac{1}{300}\right), \quad \mu_{(1,3)}^{\text{kn},0,\lambda_2,\xi_2} = \left(\frac{1}{300}, -\frac{3}{100}, \frac{3}{20}, 1, -\frac{3}{20}, \frac{3}{100}, -\frac{1}{300}\right), \\ \mu_{(3,2)}^{\text{kn},0,\lambda_2,\xi_2} &= \left(\frac{23}{4800}, -\frac{31}{2400}, -\frac{59}{960}, \frac{31}{48}, \frac{517}{960}, -\frac{319}{2400}, \frac{29}{1600}\right), \quad \mu_{(2,3)}^{\text{kn},0,\lambda_2,\xi_2} = \left(\frac{29}{1600}, -\frac{319}{2400}, \frac{517}{960}, \frac{31}{48}, -\frac{59}{960}, -\frac{31}{2400}, \frac{23}{4800}\right). \end{aligned}$$

Also the following result holds.

Proposition 12. *The use of values at five knots symmetrically distributed around a knot allows only to reproduce \mathbb{P}_4 , and this is done with the following masks:*

$$\begin{aligned} \mu_{(5,0)} &= (0, 0, 1, 0, 0), \quad \mu_{(4,1)} = \left(\frac{1}{60}, -\frac{2}{15}, 1, \frac{2}{15}, -\frac{1}{60}\right), \quad \mu_{(3,2)} = \left(\frac{7}{240}, -\frac{1}{5}, \frac{7}{8}, \frac{1}{3}, -\frac{3}{80}\right), \\ \mu_{(2,3)} &= \left(-\frac{3}{80}, \frac{1}{3}, \frac{7}{8}, -\frac{1}{5}, \frac{7}{240}\right), \quad \mu_{(1,4)} = \left(-\frac{1}{60}, \frac{2}{15}, 1, -\frac{2}{15}, \frac{1}{60}\right). \end{aligned}$$

6. Conclusion

In this paper we have proposed the construction of low-degree quasi-interpolating splines in the Bernstein basis, considering C^1 and C^2 smoothness, specific polynomial reproduction properties and different sets of evaluation points. The splines have been determined by means of masks, by setting their Bernstein-Bézier coefficients to appropriate combinations of the given data values and, in case of free parameter in the mask definition, we have imposed particular requirements, getting quasi-interpolating splines with special properties. Moreover, we have provided numerical tests showing the performances of the proposed methods.

Acknowledgment

The authors would like to thank the reviewers for their helpful comments and suggestions, which have greatly improved the manuscript. The first and third authors are members of the research group FQM 191 *Matemática Aplicada* funded by the PAIDI programme of the Junta de Andalucía, Spain. The second and fourth authors are members of the INdAM Research group GNCS of Italy. The second author acknowledges the MUR Excellence Department Project awarded to the Department of Mathematics, University of Rome Tor Vergata, CUP E83C23000330006.

References

- [1] M. Buhmann, J. Jäger, Quasi-Interpolation. Cambridge University Press, 2022.
- [2] C. Allouch, S. Remogna, D. Sbibi, M. Tahrichi, Superconvergent methods based on quasi-interpolating operators for Fredholm integral equations of the second kind, *Appl. Math. Comput.* 404 (2021) 1–14.
- [3] C. Dagnino, A. Dallefrate, S. Remogna, Spline quasi-interpolating projectors for the solution of nonlinear integral equations, *J. Comput. Appl. Math.* 354 (2019) 360–372.
- [4] S. Bouhiri, A. Lamni, M. Lamni, Cubic quasi-interpolation spline collocation method for solving convection-diffusion equations, *Math. Comput. Simul.* 164 (2019) 33–45.
- [5] R. Kumar, A. Choudhary, S. Baskar, Modified cubic B-spline quasi-interpolation numerical scheme for hyperbolic conservation laws, *Appl. Anal.* 99 (2020) 158–179.
- [6] L.Y. Sun, C.G. Zhu, Cubic B-spline quasi-interpolation and an application to numerical solution of generalized Burgers-Huxley equation. *Adv. Mech. Eng.* 12 (2020) 1–8.
- [7] J. Zhang, J. Zheng, Q. Gao, Numerical solution of the Degasperis-Procesi equation by the cubic B-spline quasi-interpolation method, *Appl. Math. Comput.* 324 (2018) 218–227.
- [8] E. Pellegrino, L. Pezza, F. Pitolli, Quasi-Interpolant Operators and the Solution of Fractional Differential Problems, *Springer Proceedings in Mathematics and Statistics* 336, 2021, pp. 207–218.
- [9] E. Pellegrino, F. Pitolli, Applications of optimal spline approximations for the solution of nonlinear time-fractional initial value problems, *Axioms* 10 (2021) 249.
- [10] F.J. Ariza-López, D. Barrera, S. Eddargani, M.J. Ibáñez, J.F. Reinoso, Spline quasi-interpolation in the Bernstein basis and its application to digital elevation models, *Math. Meth. Appl. Sci.* 46(2) (2023) 1687–1698.
- [11] A. Lamni, M.Y. Nour, D. Sbibi, A. Zidna, Generalized spline quasi-interpolants and applications to numerical analysis, *J. Comput. Appl. Math.* 408 (2022) 114100.
- [12] D. Barrera, C. Dagnino, M.J. Ibáñez, S. Remogna, Point and differential C^1 quasi-interpolation on three direction meshes, *J. Comput. Appl. Math.* 354 (2019) 373–389.
- [13] D. Barrera, C. Dagnino, M.J. Ibáñez, S. Remogna, Quasi-interpolation by C^1 quartic splines on type-1 triangulations, *J. Comput. Appl. Math.* 349 (2019) 225–238.

- [14] T. Sorokina, F. Zeilfelder, An explicit quasi-interpolation scheme based on C^1 quartic splines on type-1 triangulations, *Computer Aided Geometric Design* 25 (2008) 1–13.
- [15] R. A. DeVore, G. G. Lorentz, *Constructive Approximation*, Springer, Berlin-New York, 1993.
- [16] P. Sablonnière, Univariate spline quasi-interpolants and applications to numerical analysis, *Rend. Sem. Mat. Univ. Pol. Torino* 63(2) (2005) 107–118.
- [17] R. Franke, Scattered data interpolation: Tests of some methods, *Math. Comp.* 38 (1982) 181–200.
- [18] G.M. Nielson, A first order blending method for triangles based upon cubic interpolation, *Internat. J. Numer. Methods Engrg.* 15 (1978) 308–318.